# Radiofrequency Radiation Current Research

## Publications from 2019-2020

Kayla Dennis/Thursday 5th November, 2020/Ontario Canada

## Acronyms

Acronyms: Peripheral Blood Mononuclear Cells (PBMC), Extremely Low Frequencies (ELFs), Radiofrequency (RF), Electromagnetic Field (EMF), Electromagnetic Radiation (EMR), Reactive Oxygen Species (ROS), Microwave (MW), Reactive Oxygen Species (ROS), Specific Absorption Rate (SAR), World Health Organization (WHO), Ribonucleic Acid (RNA), Deoxyribonucleic Acid (DNA), Millimeter Wave (MMW), Microwave (MW), Magnetic Field (MF), Mesenchymal Stromal Cells (MSC), Synaptic Vesicles (SVs), Voltage Gated Calcium Channels (VGCC), Linear Model (LM)

## 1 Adverse health effects of 5G mobile networking technology under real-life conditions

There are many faults and missing avenues with current EMF research and its extrapolation to human health effects. For much of this there is a good reason. That is determining biological relevance has proven more difficult in relation to RF-EMF. Firstly, lab tests conducted on animals may be missing out on certain effects or giving false positives. This is based purely on mass differences between human beings and these animals which could result in physiological measurement differences. Inhaled and ingested substances can be scaled, radiation posits a different conundrum. For non-ionizing radiation penetration depth is a result frequency, tissue and other parameters. Therefore, the size of the organism could change the penetration depth and the effected organs. Second, the EMF signal for most laboratory settings is a single carrier frequency; the lower frequency superimposed signal containing the information was not always included. This may be important as the ELFs are always present in telecommunications and this is where some of the effects are observed. While 50% of studies do not show any effects, studies employing real life exposures display an almost 100% consistency for adverse effects. Thirdly, these lab experiments typically involve one stressor under pristine conditions. This does not emulate real life exposures with multiple toxic stimuli, in parallel over time. Roughly 5% of experiments utilized combination stressors adding either a biological or chemical toxic stimulus. As the vast majority of scientific experiments excluded either one or both of these parameters it must be reported that the current published biomedical literature is 1) extremely conservative and 2) a low 'floor' for adverse effects from wireless radiation, not the 'ceiling'. Penetration of 5G technology due to its higher frequency (at least an order of magnitude higher than 4G frequencies) is estimated to go no farther than skin deep. At these frequencies one can expect resonance phenomena with small-scale human structures. Current belief is that the peripheral structures at risk would result in skin cancer, cataracts and other skin conditions. However, the evidence suggests that biological responses can be initiated within the skin, resulting in systemic signalling within the skin causing physiological effects on the nervous system heart and immune system. Much of the data from laboratory and epidemiological studies currently available indicates that wireless networking technology have significant adverse health effects. Much of the data was obtained under conditions not reflective of real life such as:

including information content of signals, along with carrier frequencies, including other toxic stimuli in combination with wireless radiation, the adverse effects correlated with wireless radiation are increased substantially. Adding 5G into an already toxic wireless radiation environment will exacerbate the adverse health effects shown to exist. More research and testing are required[4].

## 2 Towards predicting intracellular radiofrequency radiation effects

Weak RF magnetic fields in the MHz range have been shown to influence concentrations of ROS in living cells. The energy that would be deposited by such radiation is orders of magnitude smaller than the energy of molecular thermal motion. An explanation to the observed effect would be the interaction of RF magnetic fields with transient radicals within the cells, affecting the ROS formation through radical pair mechanism 11. The prediction of the effects in biomolecular systems is not straightforward and relies on multiple interlinking scales ranging from electrons to the whole cell. See 6 & 10.

Radicals have a high reactivity rate and a plethora of pathways exists in which EMFs could interact with them. This is not novel and there are many theories that exist contemplating methods of interaction, all containing the specification of a radical pair, Hamiltonian 5. This describes how unpaired electrons interact with internal and external magnetic fields and with each other in the molecular environment. A spin model 12 was then determined for the molecules and their radical pairs 13. The computational approach has the predictive power required to evaluate the possible health effects of RF magnetic fields.

They use the Liouville-von Neumann equation 7 because it describes the groups of transient intracellular radical pairs and allows for the prediction of their response to external RF- MF. The differences in probability of the singlet state product caused by the RF field has been shown to depend on the structure of the molecular system. The computations predict that in order for significant RF-field induced effects to occur between the 1-50 MHz range the RF field strength needs to be below 100 $\mu T$. The workflow of this study 8 describes a general framework that can be applied to many different physical systems, not simply radical pairs. The remaining challenge is to identify and explain the observed RF magnetic field effects in cells, to find the cellular processes, and design experiments to obtain the magnitude of any RF field effects 9.

Therefore, calculations such as those presented within this study can be of use in explaining observed effects of RF fields and make predictions about frequency ranges that deserve experimental investigation in order to observe an effect [7].

## 3 Effect of 900-, 1800-, and 2100- MHz radiofrequency radiation on DNA and oxidative stress in brain

The researchers completed a study on rat brains and measured oxidant and antioxidant parameters in the blood and brain tissue. It was determined that it lead to increased oxidative stress and DNA damage for all three frequencies. Furthermore, 2100 MHz may lead to single strand DNA breaks as well. On top of this there are concerns that long-term exposure could lead to cumulative biological effects that have a strong correlation regarding intensity and duration of exposure. These studies focused on the frontal lobe brain tissues. See Figures 3 & 4.

Taking a quan mechanical approach, considering the biochemical reactions as both free-floating electrons as well as formation and breaking pro-

cesses of hydrogen within a medium have been responses to EMF exposure. This so called "water hypothesis" seems a more consistent explanation of the effects of EMF. As the valence angle of the O-H bond in water molecules is highly sensitive to different environmental factors as it determines the dissociation and physiochemical properties. This hypothesis posits that EMF can change the physiochemical properties of water and modulate cellular metabolism. The reaction with ROS also depends on $Ca^{2+}$ concentration in water. It has previously been determined that the effects of EMF on physiological solutions depends on the environmental medium. MW induced activation of cAMP- dependent Reverse $Na^{+}/Ca^{2+}$ exchange can have a poisoning effect on metabolism, which could be considered a negative effect on cell pathology. This exchange leads to an increase in Ca2+ which causes poisoning by inducing water influx leading to an increase of membrane permeability of $Na^{+}$.

Focussing specifically on the human brain which EMF can penetrate as deep as 4-6 cm. The brain is a high oxygen consuming organ which can cause the production of brain-ROS and a target for reactive free radicals as it includes high amounts of lipids and polyunsaturated fats. Additionally, the enzymatic defence mechanism of the brain is also relatively weak; therefore, it is susceptible to EMF-induced oxidative damage by brain-ROS. Higher levels of free oxygen and nitrogen can cause oxidative damage by attacking basic biomolecules (proteins, lipids and DNA) and cell structure. It was shown that the effect of EMF on physiochemical properties in water solutions and the formation of ROS depends on $Ca^{2+}$ concentration in the water, temperature, background radiation, light, and gas composition of the medium.

Non-thermal MW radiation can change the physiochemical properties of the skin and sub-skin water contents. Penetration of MW into the brain depends on hydration of the tissue and very little energy is absorbed by the brain. This study focused on the long-term application of RFR by GSM bands causes single-strand DNA breaks in the frontal lobe of the brain in rats, as well as the effects on oxidant and antioxidant parameters in blood or brain tissue. Short term exposure does not seem to influence ROS production. However, the longer-term exposure was found to cause an imbalance in the oxidant antioxidant relationship. This leads to damage caused by oxidative stress. The frequency of RF may affect the DNA damage in correlation with oxidative stress levels. See Figures 1 & 2 [2].

# 4 Low- Level Radio Frequency Exposure Does Not Induce Changes in MSC Biology: An in vitro Study for the Prevention of NIR-Related Damage

It has been reported that the adverse effects of RFR interacting with biological macromolecule structures can be deleterious to stem cells inducing impairment of their main functions involving self-renewal and differentiation. They studied 169 MHz on MSC administered via an open 2G "smart meter" for different duration times. The prototype Open 2G meter emits short pulses of 0.2 seconds every 2 seconds (at an unknown power level).

The biological effects related to RF exposure are broken down into three categories:

1. Interaction with biological macromolecular structures with no clinical effect
2. Reversible morphological and functional modifications in macromolecular structures with instrumentally, clinically or subjectively demonstrable effects that disappear instantaneously upon the cessation of the stimulus
3. Permanent biological damage that does

not disappear upon cessation of stimulus; wherein the biological effects exceed efficacy thresholds of damage repair, adaptation and compensatory mechanisms 31

MSCs are a good study model because they are universal in human connective tissue and contain a subpopulation of stem cells capable of differentiating into three other cell types. As the preliminary study they measured if exposure duration had any deleterious effects. It was determined that short exposure (not exceeding 1440 minutes) of MSCs to 169 MHz displayed neither loss of differentiation capacity nor increased apoptosis and ROS did not modify the biology of the MSCs 14 [1].

## 5 Trafficking of Synaptic Vesicles is Changed at the Hypothalamus by Exposure to an 835 MHz Radiofrequency Electromagnetic Field

The researchers are attempting to determine if exposure to an RF-EMF of 835 MHz at 4.0 W/Kg for 5 hr/day for 12 weeks causes changes to the SVs of the hypothalamic pre-synaptic terminals in mice. They determined that there were a great many changes to the SVs after exposure such as the following: number and size of SVs decreased, the density (numbers/$\mu m$) of docking and fusing of SVs in the pre-synaptic terminal membrane active zones decreased, the expression levels of synapsin I/II and synaptotagmin I, two regulators of SV trafficking in neurons were also significantly decreased as well as the $Ca^2+$ channel expression. These changes could directly decrease the amount of available neurotransmitters. Due to these changes the researchers studied possible phenotypical changes in body temperature, weight and olfactory response and determined there were no measurable effects in that area 15.

The industry (SAR) standard is 4.0 W/Kg exposure for limbs but it is 8-10 W/Kg to head and trunk for industry workers. In this study the whole body (mouse) experienced exposure to the 4.0 W/Kg as well as a sham control group. The mice hypothalamic slices were analysed and based on the current findings it is greatly speculated that hypothalamic neurotransmission reduction could be highly associated with 835 MHz RF-EMF. The number of SVs in the hypothalamic regions were decreased but the size was actually found to have increased in cortical and dopaminergic neurons in the striatum after exposure 16. However, the number of SVs in the medial nucleus of the trapezoid body in the auditory system actually increased. This data indicates that the different regions of the brain respond differently to RF-EMF exposures.

It has been conveyed that overexpression of synapsin Ia leads to a decrease in the size of SVs and active zones in the rat calyx of Held, thus mediating SV distribution within the synaptic terminal. Interestingly, the opposite phenotype was reported by the same group after deletion of all synapsin isoforms. This data implies that the expression levels of the synapsin proteins can regulate both SV and active zone size in presynaptic terminals.

Calcium ions play a key role in the regulation of neurotransmitter release, excitability, and synaptic plasticity. The synaptic vesicle protein SYT1 acts as a key $Ca^2+$ sensor for fast synchronous synaptic vesicle exocytosis. The calcium homeostasis in neurons can be regulated by several types of calcium channels, including VGCCs. VGCCs are responsible for fast calcium influx into the cell, which controls the entry of calcium ions across the plasma membrane. The expression of VGCCs was also significantly reduced at the hypothalamus in response to RF-EMF exposure 17. Together, the decreased expression of synapsin I/II, SYT1, and VGCCs by RF-EMF exposure may contribute to a decrease in the number

and size of the SVs in hypothalamic neurons 18.

For further investigation based on these findings the researchers studied the possible phenotypical changes in core temperature, body weight, and olfactory function but found no significant changes. Thus, they tested the possible changes in hypothalamic function because the trafficking of SVs was changed by RF-EMF exposure. The hypothalamus is part of the limbic system and is important for linking the nervous system to the endocrine system. The hypothalamus has been known to regulate critical functions such as thermoregulation, appetite, thirst, fatigue, sleep and circadian rhythms and is an important regulator of the endocrine system. Body temperature was measured during exposure rectally, there was no change in bodyweight during or after exposures compared to the sham, and the buried pellet test for olfactory response showed no differences between groups.

Therefore, the effect of the changes in SVs are not phenotypically known yet. However, it is possible that the phenotypic changes could be observed in a hypothalamic disease model because of disturbing the hypothalamic neurotransmission of disease. Future studies are needed to address this question[3].

## 6 Immunotropic effects in cultured human blood mononuclear cells exposed to a 900 MHz pulse-modulated microwave field

PBMCs were chosen as an appropriately sensitive detector as part of the homeostatic neuro-endocrine-immune network. Since EMF may influence the organism in an extremely subtle way, and the immune systems reacts to discrete environmental stimuli it is the perfect biological system to investigate 19. More precisely to observe lymphocyte proliferation. The immune response to EMF at 900 MHz pulsed radiation is measured via lymphatic response from the blood of healthy donors 22. The samples were exposed to 20 V/m, SAR of 0.024 W/kg twice for 15 min each and compared to a control 20. They found after the initial dose a higher LM index (immunogenic activity) and T-cell response to concanavalin A; however, this decreased after the second dose. The interleukin-2 (IL-2) saturation rose after the second dose, and mitogen response dropped. This suggests that PBMC can overcome stress caused by mitogens after exposure to 900 MHz radiation. These types of studies vary wildly from epidemiological studies in that it is too expensive and time consuming to measure and test a true environment. There are too many signal types and sources to measure and quantify them all in one study. The researchers suggest adding cytokine and chemokine to the observable changes, as well as different RF-EMF models. The findings determined that lymphocytes and monocytes are sensitive to 900 MHz EMF 21. Also, that EMF exposure may help mitogen-activated cells to overcome cellular stress; however, the mechanism is yet unknown [10].

## 7 Global gene expression analysis of Escherichia coli K-12 DH5 alpha after exposure to 2.4 GHz wireless fidelity exposure

EMF influences all living cells not just human beings, this is study observes its effects on bacteria, specifically E-coli O157H7 23. It has previously been determined that among the non-thermal effects of EMF are increased antibiotic resistance (declared a “global health crisis” by WHO), motility and an ability to form a biofilm. In this study it was found that from the RNA-seq

experiments on 101 genes it was determined that 52 genes are up-regulated and 49 are down-regulated. EMF exposure induced different responses in the bacteria depending on the frequency, intensity and exposure time of the organism model, with a large variety in all aspects 24. Some bacteria with multidrug resistance were found near telecommunication stations. The microbial growth of the microbiota on human skin was also disturbed after RF-EMF exposure. The cellular mechanisms and areas affected are the following: locomotion, localization of cell, bacterial-type flagellum-dependent cell motility, chemotaxis, response to external stimulus and chemicals, cell adhesion, cellular component organization or biogenesis, DNA repair and metabolism, nucleotide biosynthetic process, carbohydrate derivative metabolic process, organonitrogen compound metabolic process. The findings that Wi-Fi exposure increased motility of E. Coli O157H7 by 28%, which may be the pathogens strategy for survival after excessive stress exposure. Previously, it has been reported that Wi-Fi exposure triggers biofilm formation, via induced expression of padG, yadM, yadC and fimI involved in cell adhesion as well as yciG involved in flagellum-dependent swarming motility. These changes permit the survival in environments with rapidly changing conditions. It was found that genes involved in both aerobic and anaerobic respiration were down-regulated after Wi-Fi exposure, meaning that decreased metabolic activity is linked to increased persistence. Most of the down-regulated genes were involved in cell cycle, metabolism and transport. Conversely, the up-regulated genes were associated with stress response and apoptosis. Exposure also influenced the transcription of a network of regulatory genes that affected several biological processes. Further research is required to clarify if these findings are consistent and could lead to further studies on the mechanisms by which EMF influences the bacterial transcriptome, and what effects it could have on human health and disease. Undervaluing the problem of telecommunication exposure could lead to a further rise in infectious diseases and their complications [8].

# 8 Radiofrequency electromagnetic radiation-induced behavioural changes and their possible basis

As the telecommunication industry is growing rapidly, science is having a difficult time keeping up with the possible health effects research. The long-term consequences of non-ionizing radiation are yet to be fully understood. Among this is the behavioural studies for learning, memory, anxiety and locomotion. A literature analysis on the behavioural effects of RF-EMF reveals a complex picture with conflicting observations. This study presents the current findings for the possible neural and molecular mechanisms for the behavioural effects 25.

Upon review the author determined that exposure to RF-EMR induces changes in the oxidant/antioxidant defence system of the brain which is indicative of the internal environment of each brain cell being disturbed via the RF insult. Thus, leading to improper function of the cell, and when a threshold is reached the cell either stops functioning, functions abnormally or dies. This is known as either structural or morphological change. Most of the time changes that happen at the cellular level become evident at the behavioural level, but it is difficult to link up structural and morphological changes to behavioural changes. Biochemical homeostasis imbalances will result in behavioural changes, but there may be no evidence of structural change or vice versa. Mechanisms that prevent and resist insult changes from external stressors are a reason these mechanisms are difficult to observe during RF-EMF exposure. There is evidence of behavioural effect changes after exposure in rodents but extrapolation to humans is difficult.

Estimations of human exposure are often greater than those of rodent studies, and behavioural studies in young adults are scanty. Although the current study focused on RF-EMR induced effects on cognition, anxiety and locomotion there is evidence of other RF-EMR induced behavioural effects in rodents as well as humans [6].

# 9 5G Wireless Communication and Health Effects- A Pragmatic Review Based on Available Studies Regarding 6 – 100 GHz

The researchers did a review of current literature focussing on the in vivo and in vitro studies studying 6-100 GHz publications. These 94 publications were then sub-categorized into biological materials (cell type, species etc.), biological endpoint, exposure (duration, frequency and power), and results. They found that 80% of in vivo studies showed a response in relation to exposure, while 58% of in vitro studies demonstrated an effect. All biological endpoint studies showed a response. They found no consistent relation between power density, exposure duration, frequency and exposure effects 26.

Surprisingly very few studies were found to be within the lower frequency ranges (6-30 GHz) as these are the most frequently found in use and contain some of the new 5G frequencies that will/are implemented. The analysis of the studies performed was based on publications/studies not actual experiments (there can be multiple experiments in one study). The report does not contain a statistical analysis of exposure conditions and results. The reason for many of the studies was for the use of RF-EMF in medicinal therapy. Therefore, the frequencies and often power levels were based on the machines used in that. These studies were conducted with the aim of determining medical relevance. As can be seen by the majority of the studies conducted within the 40-65 GHz frequency ranges with incredibly high-power levels. These are not associated with real world exposures.

There are very few (if any) independent replication studies completed to determine the accuracy of reported results. It should also be noted that there is no trend towards classic dose-response pattern where a higher dose results in greater effects. Since studies showing tissue warming show no greater effect below than below the guideline $(1mW/cm^2)$, this would either mean that the same interactions are present at all power densities tested or that experimental artefacts unknown to scientists are present. Therefore, they determine that temperature control is the most important physical parameter. It has been consistently neglected in studies, and although temperature measurements have been reported it does not mean that biological material temperature was considered. It has been considered that the "bulk" heating can differ from what occurs at a rather limited point "hot spot". In addition, the intensity of a short burst can be lost if the measurements are based on average exposure times.

Since the ranges up to 30 and above 90 GHz are sparingly represented the review mainly covers the 30.1-65 GHz range. In summary the majority of the studies with MMW exposure found biological effects. From this observation; however, no in-depth conclusions can be drawn. There does not seem to be a consistent relationship between power density, exposure time, frequency and biological effects. Rather shockingly, higher power densities do not cause a more frequent response. Many of the studies refer to their findings as a "non-thermal" response but do not accurately apply thermal controls. The question remains, if warming is the main cause of MMW observed effects?

The following conclusions were made:

1. There can be no conclusions drawn from

6-100 GHz MMW exposures not exceeding current safety standards due to no clear evidence in the contradictory findings of in vivo and in vitro studies
2. Regarding "non-thermal" effects, studies provide no clear explanation of mode of action for observed effects
3. Regarding the quality of presented studies, too few fulfil the minimum quality criteria to allow for further conclusions 27

The study does not find adequate information to perform a safety assessment or propose safety levels, or non-thermal effects. They inform that in order to assess safety and re-structure proposed power levels study implementation needs to be significantly improved [9].

## 10 Funding Source, Quality of Publications and Outcome in Genetic Damage in Mammalian Cells Exposed to Non-Ionizing Radiofrequency Fields

The Authors observe the current literature and its funding sources combined with the findings. As this is a controversial topic caution must be taken when discussing the observations. This study consisted of 225 publications with a total of 2,160 genetic assessment tests for the effects of RF energy damage on mammalian cells. One finding was that a majority of researchers claimed government funding (53%, 120 of the 225), while only a small number acknowledged mobile industry funding (9%, 20 of the 225 publications) 28. There were many investigators who did not mention a funding source (26%, 58 of the 225). The authors noted that the telecommunication industry funded studies were of better control as they utilized proper quality control measures. These measures included blind evaluation, adequate description dosimetry, positive/sham controls compared to those funded by the government. The industry funded studies also had a consistently lower d value (difference between cells exposed and sham exposure). The percentage of finding no difference between exposed and control cells were higher for industry compared to government funded studies (80% versus 49%) and less likely to report an increase in damage (10% versus 23%). The most important note is that studies need state their funding sources and to include quality control measures.

The interpretation of results on the effects of RF radiation on health should take sponsorship into effect. This was stated by an earlier systematic review as well, as sponsorship has been known to cause observation bias. Therefore, a method of looking into possible bias is to observe the methodology. Does the research include four quality control measures? These measures include: 1) use of "blind" evaluations (B or nB) 2) adequate/detailed description of dosimetry (D or nD) 3) inclusion of "positive controls" in experiment 4) inclusion of "sham exposure" controls (S or nS) 29. The observations for this study were quality control measures and d value (effect size or standardized mean difference between cells exposed to RF energy and sham control cells.

The authors conclude that in order to alleviate "biased" discussion/debates on the efficacy of studies for the effects of RF exposure on health it is important to include funding sources in publications 30. Furthermore, it is important to not only include the quality control measures but to mention them in the publication for quality assessment. Good-quality publications are essential for national and international organizations to assess the potential health risks of RF energy [11].

Figure 1: Testing Methods Structure

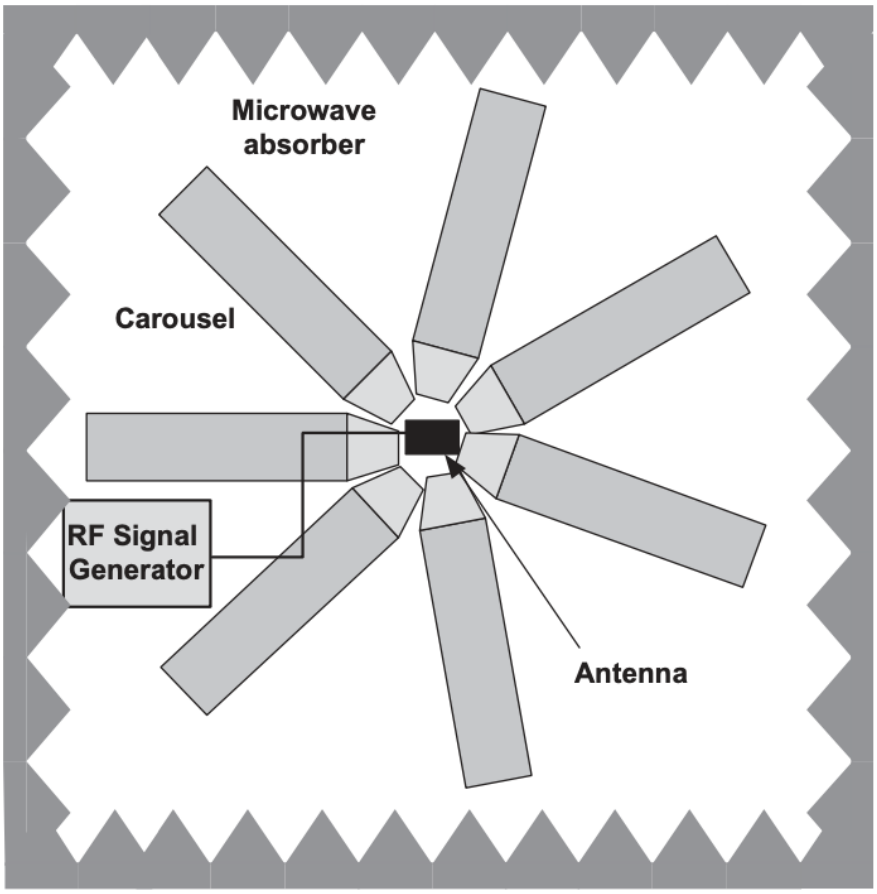


**Figure 1.** RFR experimental setup.

Figure 2: SAR Distribution of different frequencies

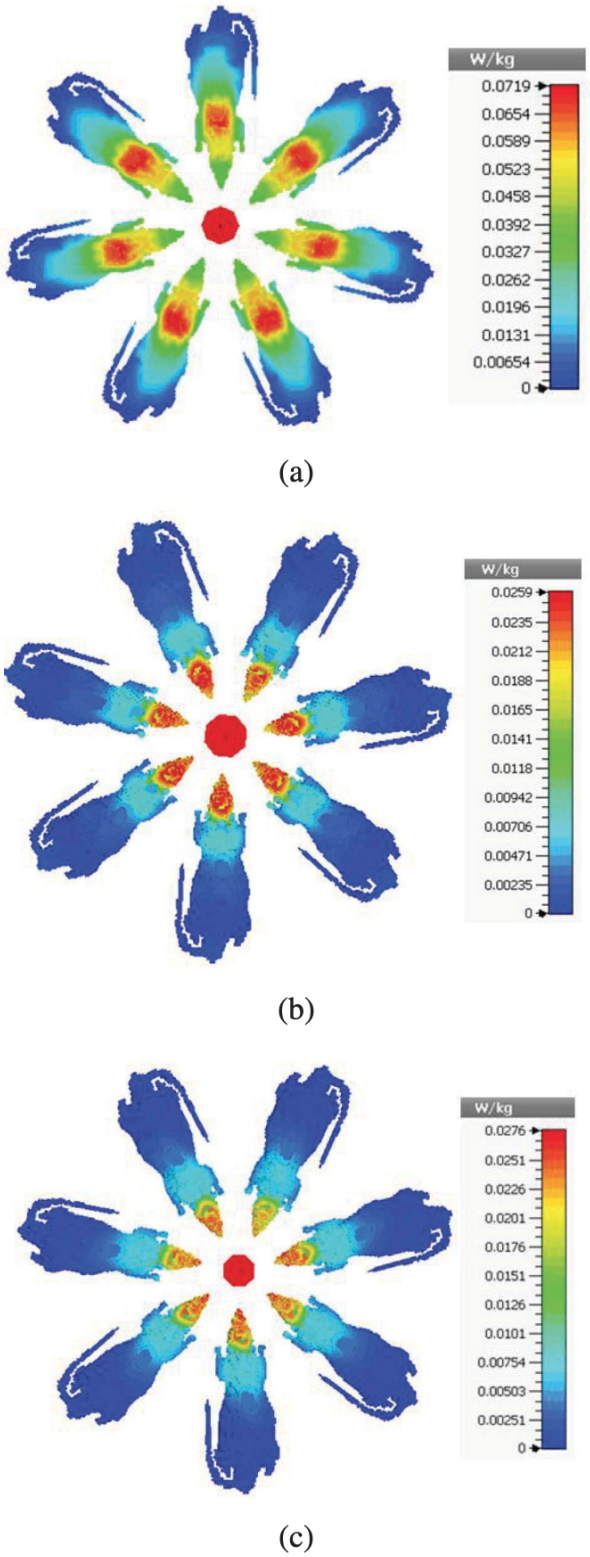


**Figure 2.** SAR distribution for 10 g average: (a) 900 MHz, (b) 1800 MHz, and (c) 2100 MHz.

Figure 3: Frontal Lobe Levels

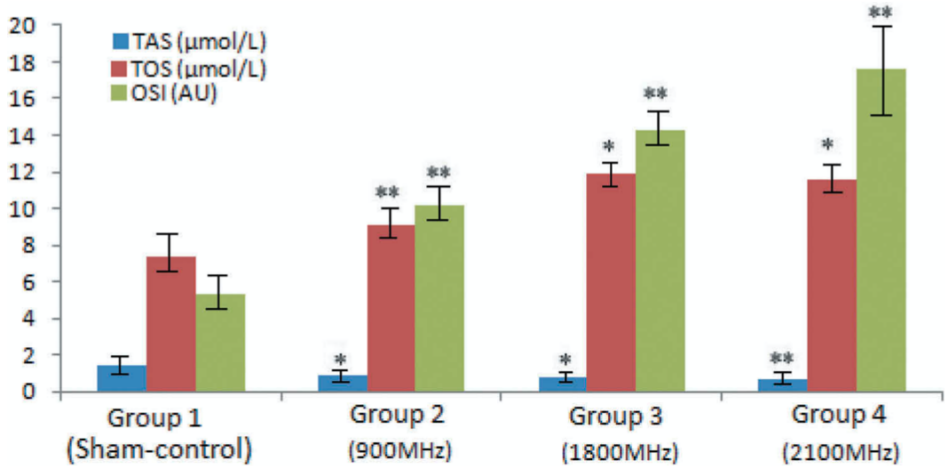


**Figure 5.** Showing TAS, TOS, and OSI levels in the frontal lobe of the brain of rats exposed to long-term (2 h/day, 6 months) RFR emitted by generators that generate signals similar to three different RF frequencies and sham-control. Values are given as Avg. ± SD (*significant compared to the control group ($p < 0.01$); **significant compared to both the control group and other groups ($p < < 0.01$)).

Figure 4: Frontal Lobe Levels



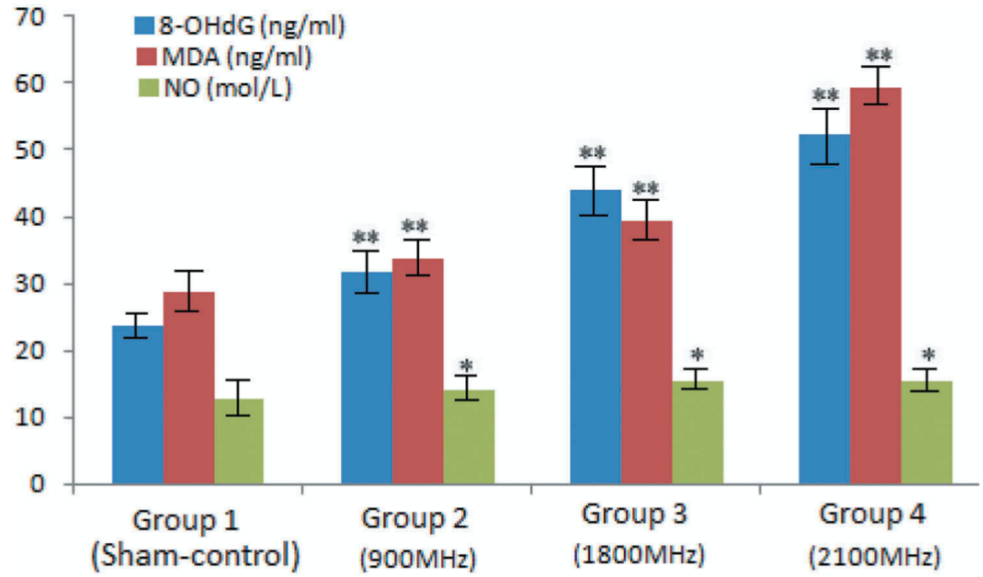


**Figure 6.** Showing 8-OHdG, MDA, and NO levels in the frontal lobe of the brain of rats exposed to long-term (2 h/day, 6 months) RFR emitted by generators that generate signals similar to three different RF frequencies and sham-control. Values are given as Avg. ± SD (*significant compared to the control group ($p < 0.01$); **significant compared to both the control group and other groups ($p < 0.01$)).

Figure 5: Hamiltonian Equation

The Zeeman Hamiltonian in Eq (6) may look rather complicated, and it is therefore instructive to write the static and RF contributions explicitly:

$$\begin{aligned}\mathbf{H}_{Z,B_0}(t,\Omega) &= g\mu_B B_0\left(R_{zx}(\mathbf{S}_{1x}+\mathbf{S}_{2x})+R_{zy}(\mathbf{S}_{1y}+\mathbf{S}_{2y})+R_{zz}(\mathbf{S}_{1z}+\mathbf{S}_{2z})\right),\\ \mathbf{H}_{Z,B_1}(t,\Omega) &= g\mu_B B_1[(R_{xx}(\mathbf{S}_{1x}+\mathbf{S}_{2x})+R_{xy}(\mathbf{S}_{1y}+\mathbf{S}_{2y})+R_{xz}(\mathbf{S}_{1z}+\mathbf{S}_{2z}))\cos(\omega t+\phi)\\ &\quad +(R_{yx}(\mathbf{S}_{1x}+\mathbf{S}_{2x})+R_{yy}(\mathbf{S}_{1y}+\mathbf{S}_{2y})+R_{yz}(\mathbf{S}_{1z}+\mathbf{S}_{2z}))\sin(\omega t+\phi)]\,.\end{aligned} \tag{7}$$

Here $R_{ij}$ are the components of the rotation matrix, $\mathbf{R}(\Omega)$, where the orientation $\Omega$ has been omitted for clarity. In the special case where the molecular reference frame is the same as the laboratory reference frame, the rotation matrix becomes the identity operator, where $R_{xx} = R_{yy} = R_{zz} = 1$, while all other components are zero. In this case Eq (7) reads as:

$$\begin{aligned}\mathbf{H}_{Z,B_0}(t,\Omega) &= g\mu_B B_0\left(\mathbf{S}_{1z}+\mathbf{S}_{2z}\right),\\ \mathbf{H}_{Z,B_1}(t,\Omega) &= g\mu_B B_1[(\mathbf{S}_{1x}+\mathbf{S}_{2x})\cos(\omega t+\phi)+(\mathbf{S}_{1y}+\mathbf{S}_{2y})\sin(\omega t+\phi)]\,.\end{aligned} \tag{8}$$

Figure 6: Methods Frame

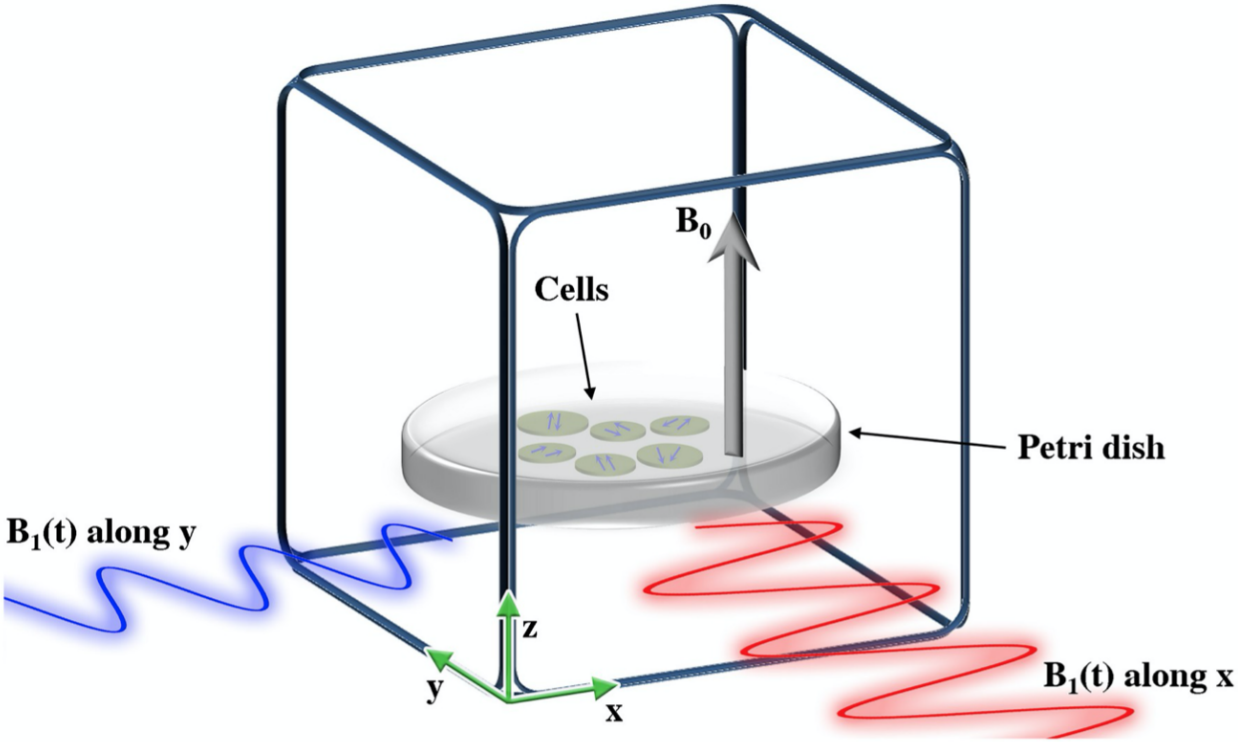


**Fig 3. The laboratory coordinate frame.** An artistic representation of a Petri dish with an ensemble of cells, and a magnetic field, $B_0$, in the direction perpendicular to the plane of the Petri dish. The Petri dish is surrounded by rectangular coils that can produce an oscillating magnetic field $B_1$ along any of the three axes in the laboratory frame. Thus an RF magnetic field rotating in the plane of the Petri dish could be produced, cf. Fig 2A. The orientation of each cells, and hence also of any radical inside the cells, is random, which dictates that any orientational dependent property of the radical pairs should be averaged over all the possible radical orientations.

Figure 7: Liouville von Neumann Equation

The dynamics of the radical pair can be described in terms of the density operator, $\rho(t, \Omega)$, and its time evolution is described by the Liouville-von Neumann equation [9, 15, 52, 55–58]:

$$\frac{\partial \rho(t,\Omega)}{\partial t} = -\frac{i}{\hbar}[\mathbf{H}(t,\Omega), \rho(t,\Omega)]_- - \frac{k_S}{2}[\mathbf{P}_S, \rho(t,\Omega)]_+ - \frac{k_T}{2}[\mathbf{P}_T, \rho(t,\Omega)]_+ . \tag{9}$$

Figure 8: Study Workflow

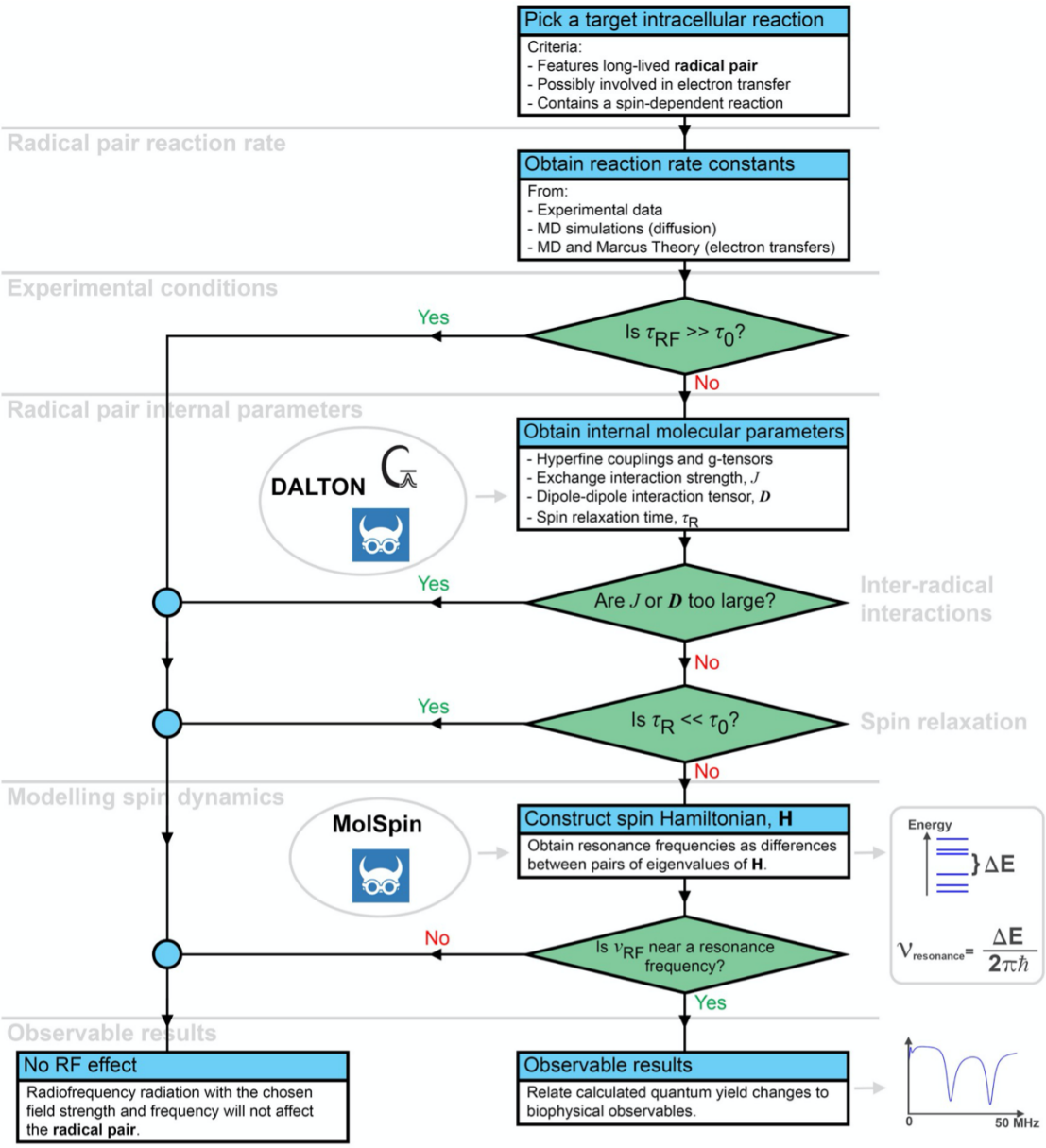


**Fig 1. An overview of the workflow to interpret intracellular RF field effects.** Three characteristic times are important to expect any possible RF field effects in an intracellular radical pair system: $\tau_0$ is the lifetime of the radical pair; $\tau_{RF}$ is the characteristic time of RF magnetic field action on the radical pair, defined in Eq (2); and $\tau_R$ the spin relaxation time. $\nu_{RF}$ is the frequency of the RF field. The steps of the workflow are discussed in the sections of text indicated on the left side of the figure.

Figure 9: RF Effects Characterization

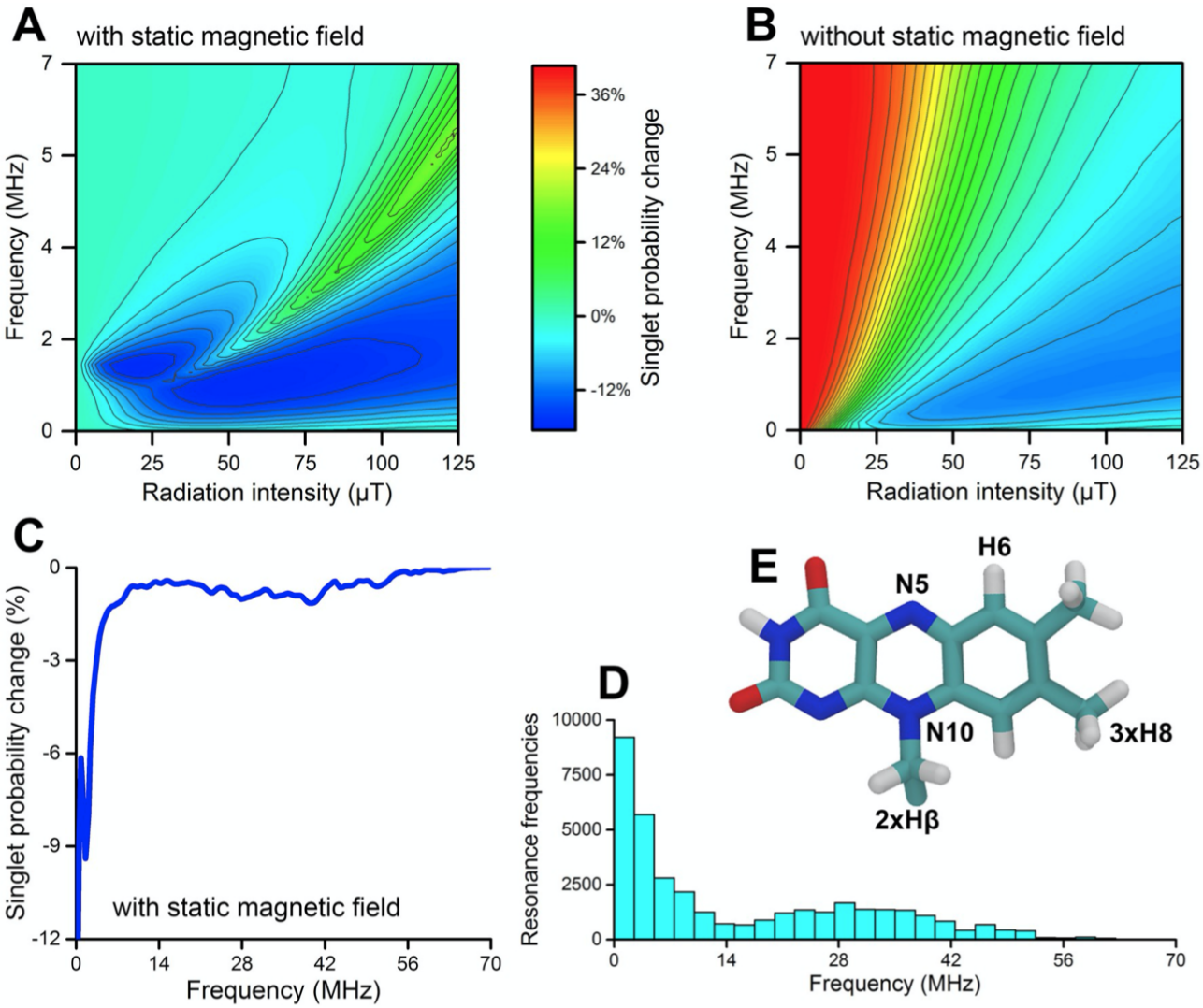


**Fig 8. Characterization of RF effects in the $[FAD^{\bullet -} \ldots O_2^{\bullet -}]$ radical pair. A-C**: The singlet product probability change was calculated for a model including 8 isotropic hyperfine interactions on $FAD^{\bullet -}$ and none on $O_2^{\bullet -}$, with (**A** and **C**) or without (**B**) a static external magnetic field of $B_0 = 50\ \mu$T along the $z$-axis. All calculations assumed $k_S = k_T = 1\ \mu s^{-1}$. Once the static external magnetic field is present, significant singlet probability changes are only seen for RF frequencies below 7 MHz as illustrated in **C**. **D**: The resonance frequencies of the system calculated from the eigenvalues of the spin Hamiltonian. **E**: The nuclei N5, N10, H6, 3 × H8 and 2 × H$\beta$ on FAD were used.

Figure 10: Singlet Change

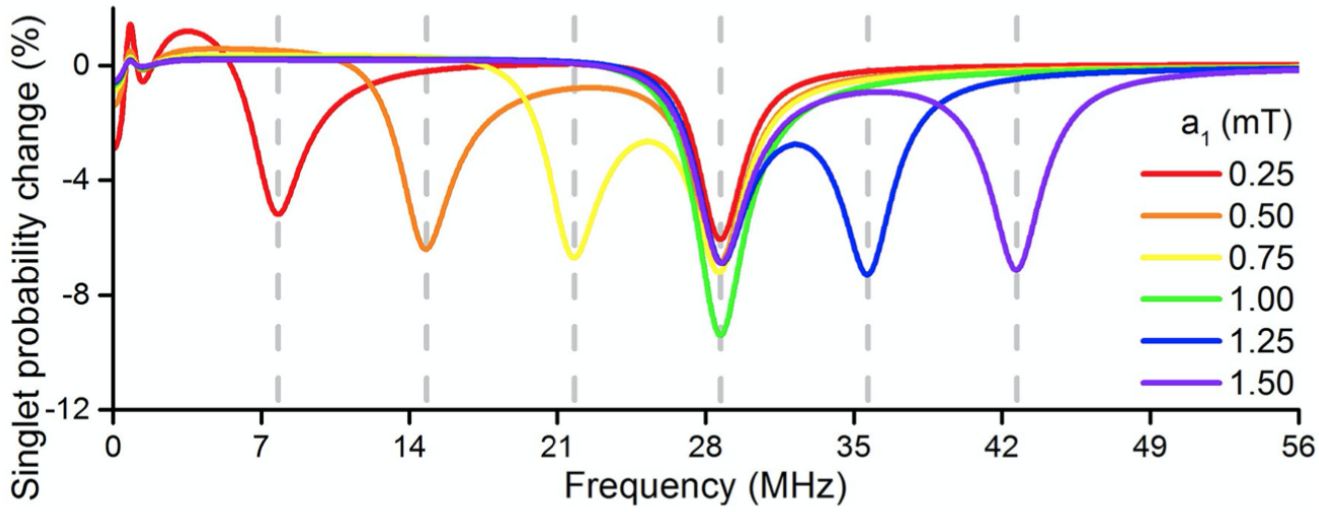


**Fig 5. Hyperfine interactions impact the singlet product probability change in the studied model reaction.** The strength of the isotropic hyperfine coupling constant $a_1$ is modified here. Pronounced changes in the singlet probability are always seen in the low-frequency limit, and for $\omega \approx a_1 \cdot 28 \frac{\text{MHz}}{\text{mT}} + 0.7$ MHz. The fixed hyperfine coupling, $\mathbf{a}_2$, gives rise to a singlet probability change around 28.7 MHz and enhances the singlet probability change at 28.7 MHz when $a_1$ = 1.00 mT. $k_S = k_T = 10^6$ s$^{-1}$, $B_0$ = 50 $\mu$T and $B_1$ = 50 $\mu$T are assumed in all calculations.

Figure 11: RF Field Equation

$$\tau_{RF} = \frac{2\pi\hbar}{g\mu_B B_1}$$

Figure 12: Spin Model

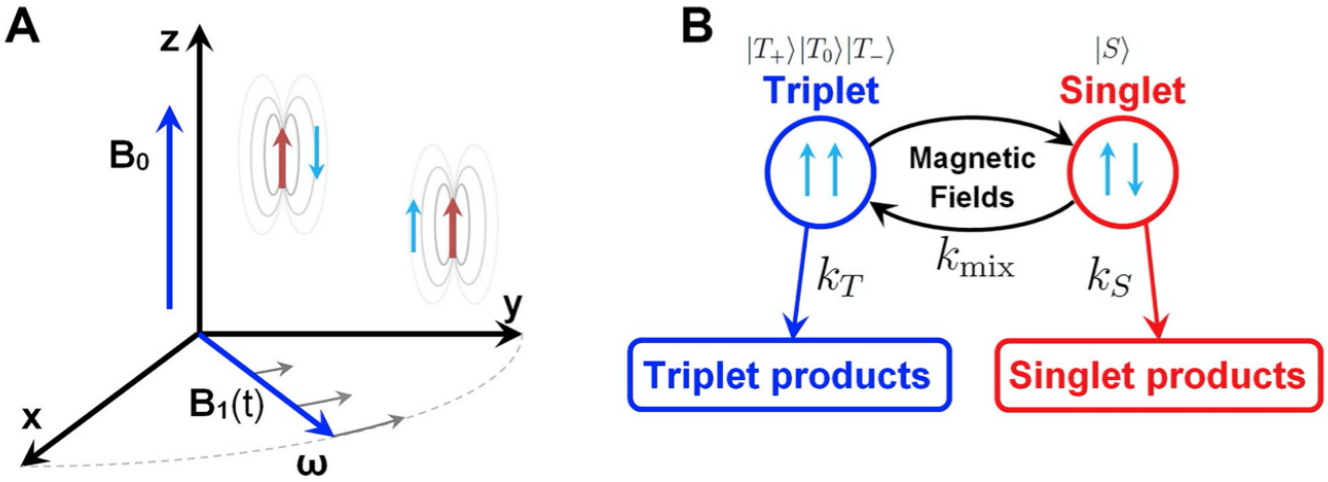


**Fig 2. Overview of the simple radical pair model. A**: The static magnetic field $\mathbf{B}_0$ points along the $z$-axis, and the RF field $\mathbf{B}_1(t)$ acts in the $xy$-plane. The unpaired electrons are each localized around the magnetic nuclei. **B**: Magnetic interactions in the system induces singlet-triplet mixing within the radical pair with a characteristic rate constant $k_{\text{mix}}$. Chemical reactions can occur with rate constants $k_S$ and $k_T$ from radical pairs in the singlet and triplet state, respectively, limiting the lifetime $\tau_0$ of the radical pair.

Figure 13: Interradical Interaction Equation

$$\mathbf{H}_{ex} = -2J(\mathbf{r})\,\mathbf{S}_1 \cdot \mathbf{S}_2, \tag{3}$$

$$\mathbf{H}_{dd} = \frac{g_1 g_2 \mu_0 \mu_B^2}{4\pi}\left(\frac{3(\mathbf{S}_1 \cdot \mathbf{r})(\mathbf{r} \cdot \mathbf{S}_2)}{|\mathbf{r}|^5} - \frac{\mathbf{S}_1 \cdot \mathbf{S}_2}{|\mathbf{r}|^3}\right) = \mathbf{S}_1 \cdot \mathbf{D}(\mathbf{r}) \cdot \mathbf{S}_2\,. \tag{4}$$

Figure 14: RF Effects on MSCs Study Findings

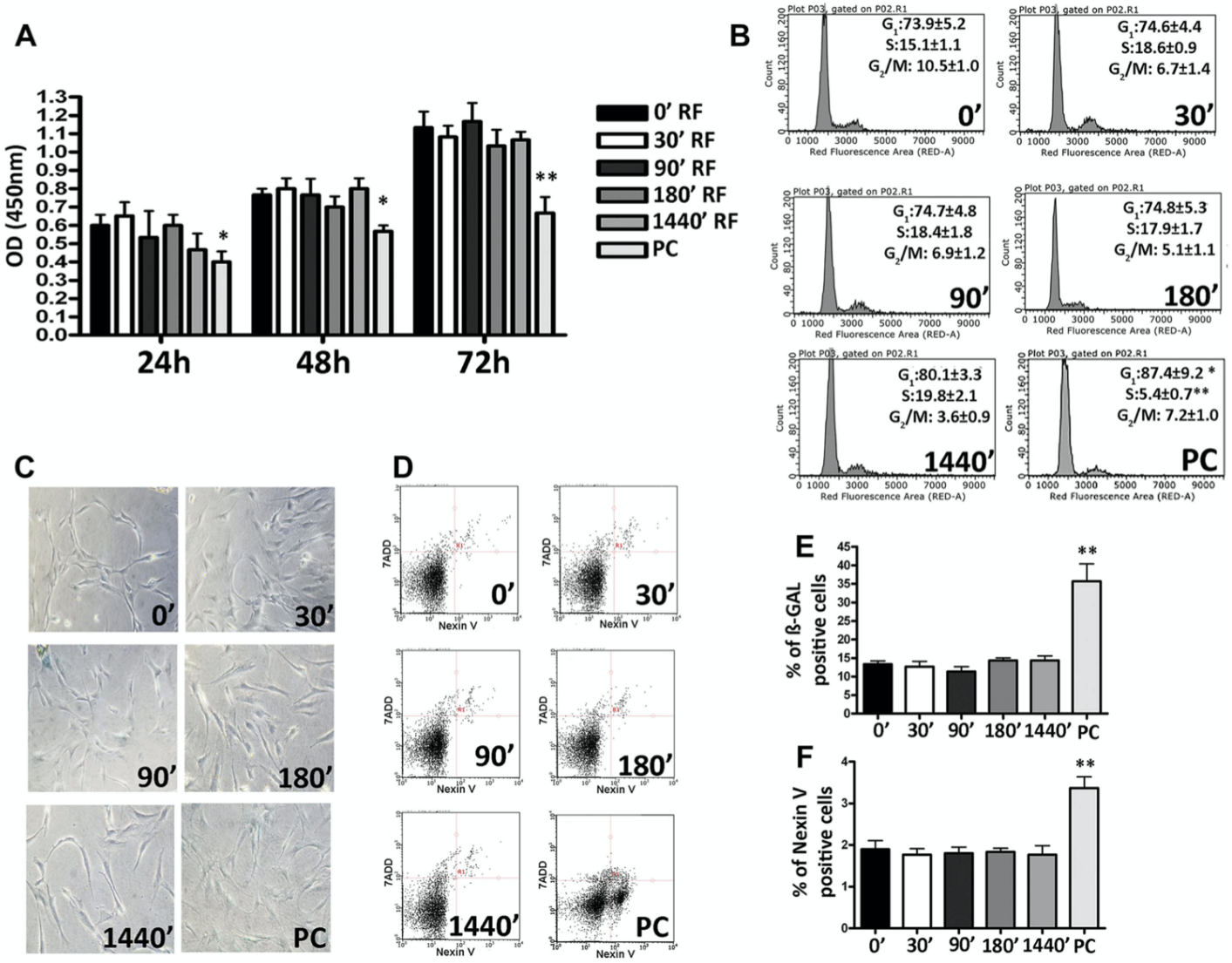


**Figure 1** Biological properties of Mesenchymal Stem Cells (MSCs) after different exposure time at Radiofrequency (RF) of 169MHz and relative positive control (PC). (**A**) Cell proliferation measured by Cell Counting Kit-8 24, 48 and 72 h after RF exposure. The graph shows the mean values ± SD (n=3, *p<0.05, **p<0.01). (**B**) The picture shows representative FACS analysis of MSCs after RF exposure. Experiments were conducted in triplicate for each condition. Percentages of different cell populations (G1, S, and G2/M) are indicated. Data are expressed with standard deviation (n=3* p<0.05, **p<0.01). (**C**) The picture shows representative microscopic fields of senescence-associated beta-galactosidase-positive cells (blue) under different experimental conditions. (**D**) The pictures show representative annexin-V analysis of MSCs after RF exposure for each condition. The assay allows the identification of early (Annexin V+ and 7-ADD–), late apoptosis (Annexin V+ and 7-ADD+) and necrotic cells (Annexin V– and 7-ADD +). (**E**) The histograms show the percentage of senescent cells in MSCs after RF exposure. Data are represented as mean ± standard deviation (SD) of three independent replicates (n=3, ± SD, **p<0.01). (**F**) The graph showed the percentage of early and late apoptotic cells. The experiments were conducted in triplicate for each condition (n=3, ± SD, **p<0.01).

Figure 15: RF Effects Body Temperature

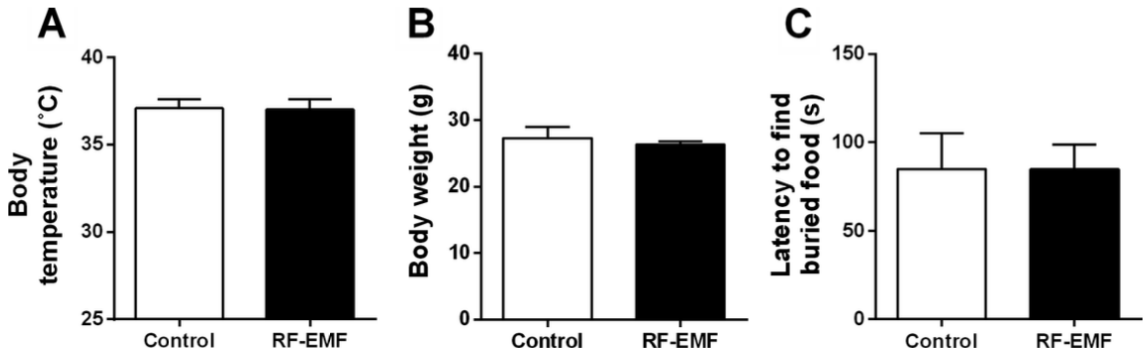


**Figure 5.** Core body temperature (**A**), body weight (**B**) and behavioral test of food finding (**C**) after 12 weeks 835 MHz RF-EMF exposure. No significant changes were seen between controls and the RF-EMF group ($n = 8$).

Figure 16: Synaptic Vesicle Number and Density

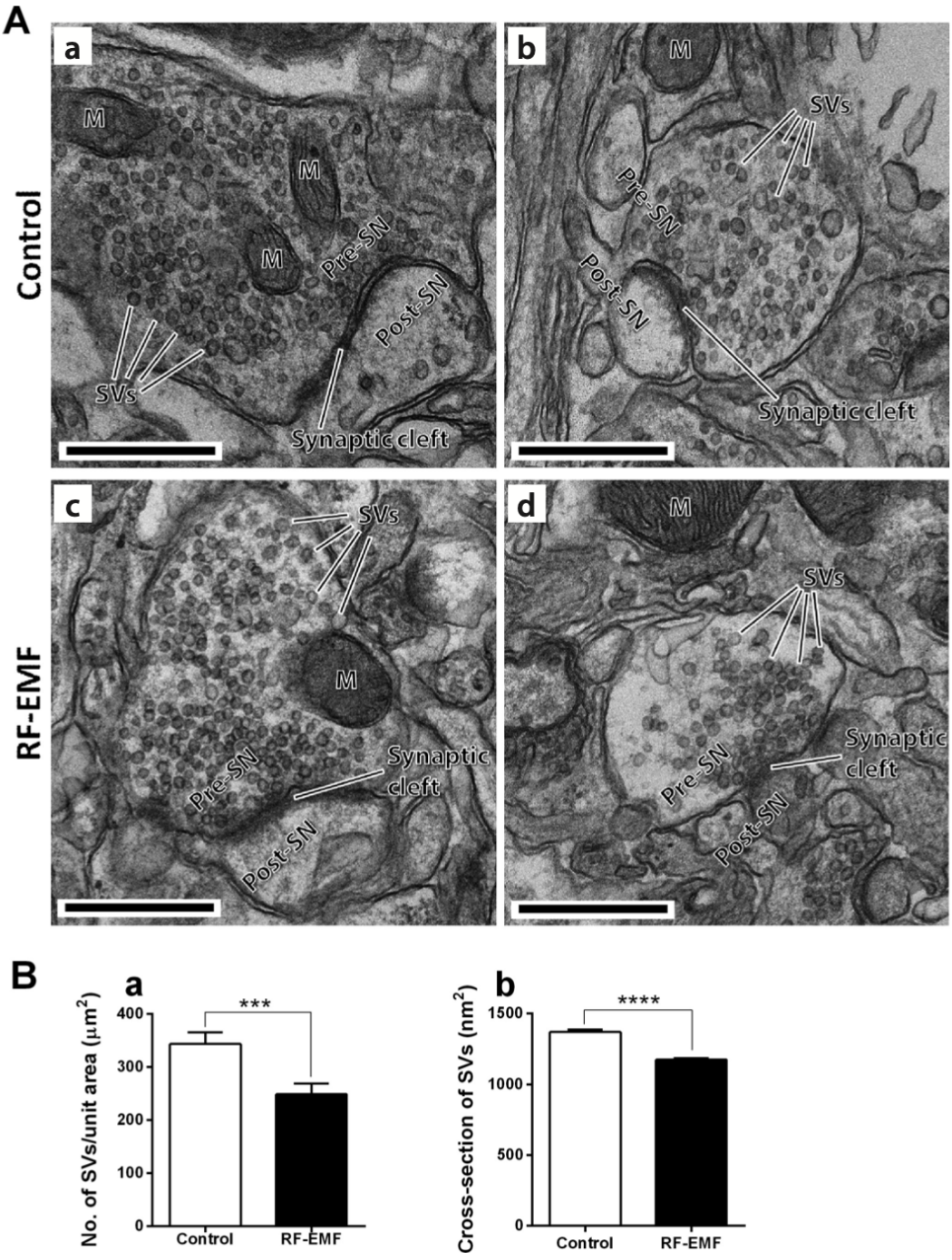


**Figure 1.** Number and size of the synaptic vesicles at the presynaptic boutons of the hypothalamic neurons. **A.** Representative TEM (transmission electron microscopy) micrographs of the synapse region in hypothalamic neurons of sham exposed (**a** and **b**) and RF-EMF exposed mice (**c** and **d**). M, mitochondria; Pre-SN, presynaptic neuron; Post-SN, post synaptic neuron; SVs, synaptic vesicles; scale bar size: 0.5 μm. **B.** Comparisons of the synaptic vesicle numbers (**a**; SVs /unit area ($\mu m^2$)) and size (**b**; the cross-section area ($nm^2$)) at the presynaptic nerve terminals of the hypothalamic neurons. Each bar represents the mean ± SEM. Statistical significance was evaluated by using a two-tailed unpaired Student's *t*-test. *** $p < 0.001$, **** $p < 0.0001$ ($n = 5$).

Figure 17: Synaptic Voltage Gated Calcium Channels

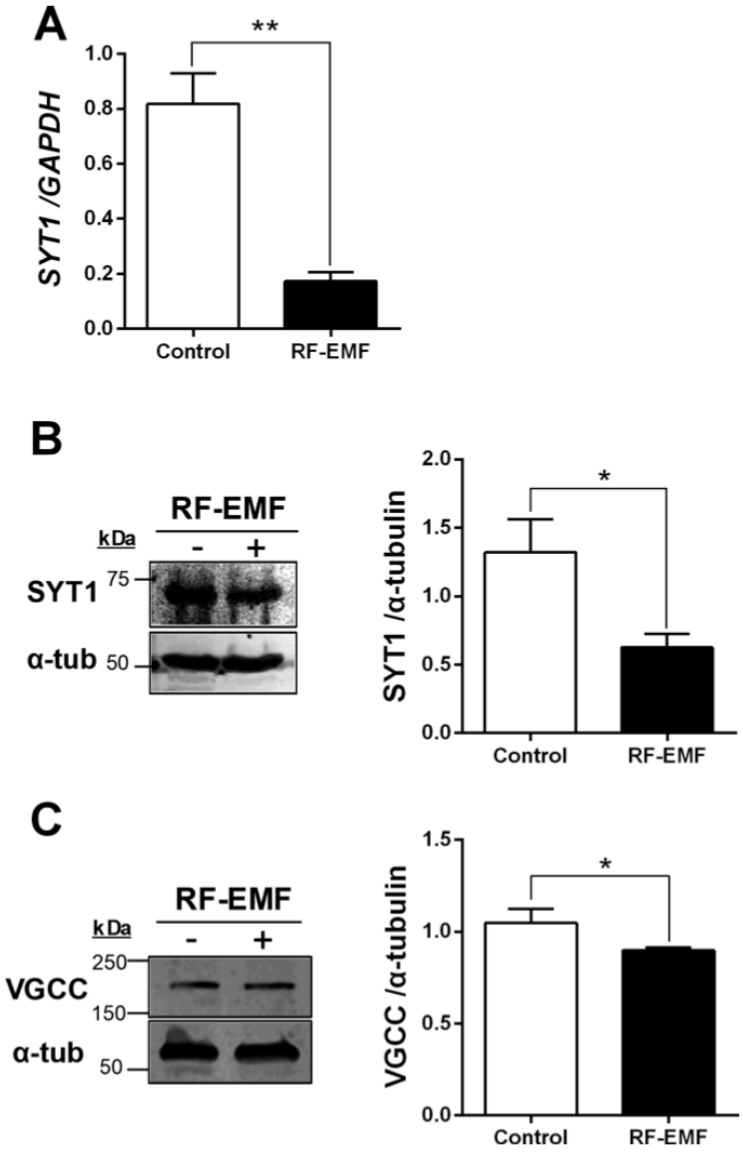


**Figure 4.** Expression changes of synaptotagmin 1 and voltage gated calcium channel in the hypothalamus after exposure to RF-EMF for 12 weeks. **A.** Hypothalamic expression levels of synaptotagmin I (SYT1). Relative mRNA level of SYT1 was significantly decreased by exposure to RF-EMF. **B.** Representative blotting images of SYT1. The expression levels of SYT1 protein in the hypothalamus were significantly decreased by RF-EMF exposure. **C.** Representative blotting images of voltage gated calcium channels (VGCC). The expression levels of VGCC in the hypothalamus were significantly decreased by RF-EMF exposure. Each bar represents the mean ± SEM. Statistical significance was evaluated by using a two-tailed unpaired Student's *t*-test. * $p < 0.05$, ** $p < 0.01$ ($n = 5$).

Figure 18: Expression of Synapsin I & II

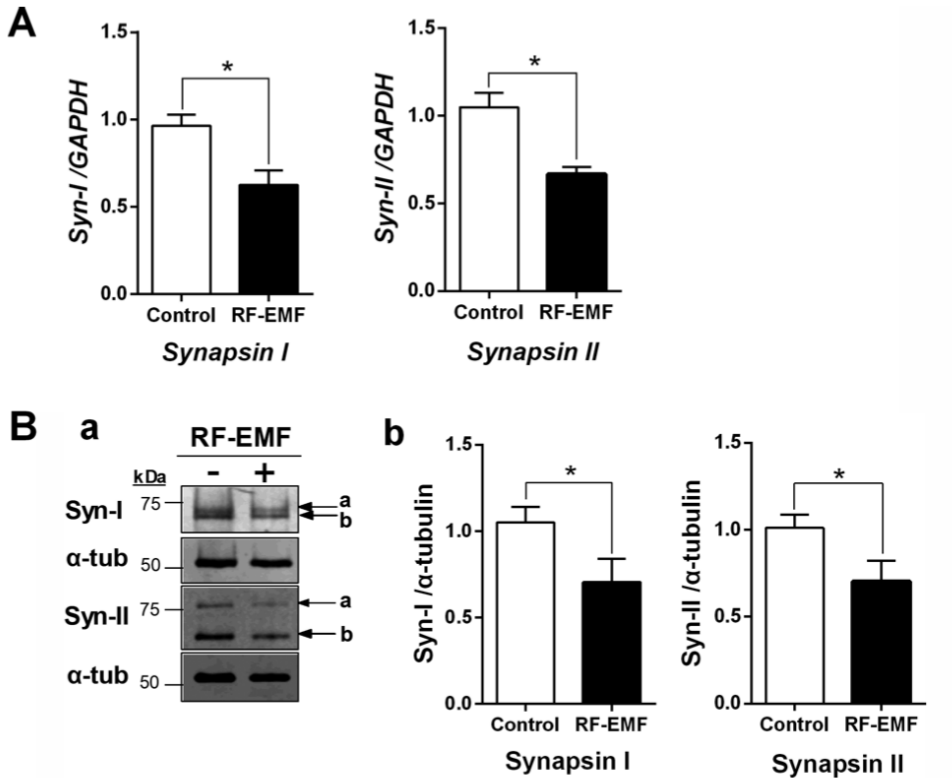


**Figure 3.** Expression changes of synapsin in the hypothalamus after exposure to RF-EMF for 12 weeks. **A.** Hypothalamic expression levels of synapsin I and synapsin II. Relative mRNA levels of synapsin I/II were significantly decreased by exposure to RF-EMF. **B.** Representative blotting images of synapsin I/II (**a**). Hypothalamic synapsin I and synapsin II protein levels were significantly reduced by RF-EMF exposure (**b**). Each bar represents the mean ± SEM. Statistical significance was evaluated by using a two-tailed unpaired Student's *t*-test. * $p < 0.05$ ($n = 5$).

Figure 19: Experimental Methodology

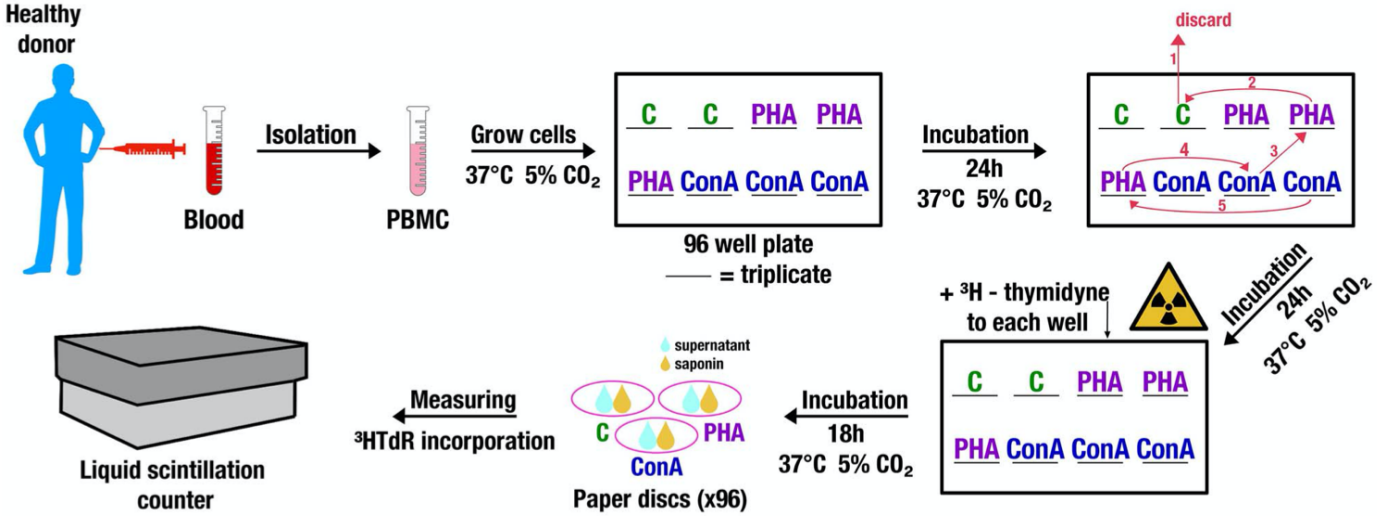


**Fig. 1. Schematic representation of performed experiment. PBMC= peripheral blood mononuclear cells, C= control, PHA= phytohemagglutinin, ConA= concanavalin A.**

Figure 20: Experimental Chamber: Created for this experiment

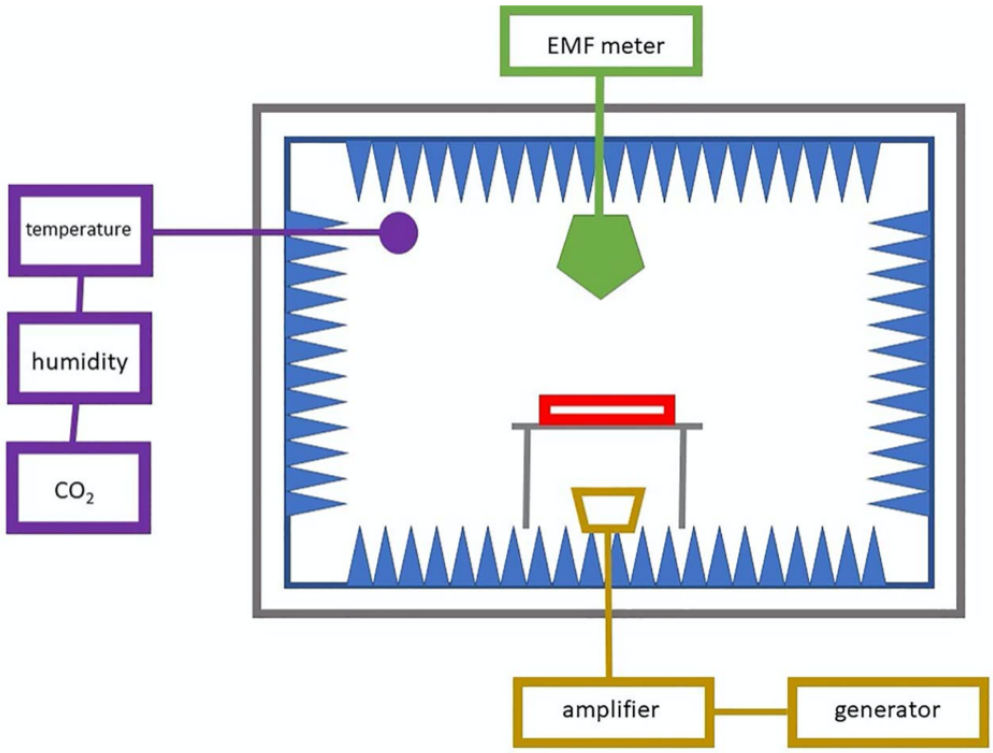


**Fig. 2. Schematic diagram of a minature anechoic climate chamber for cell culture exposure to electromagentic field.**

Figure 21: Results for T Lymphocytes

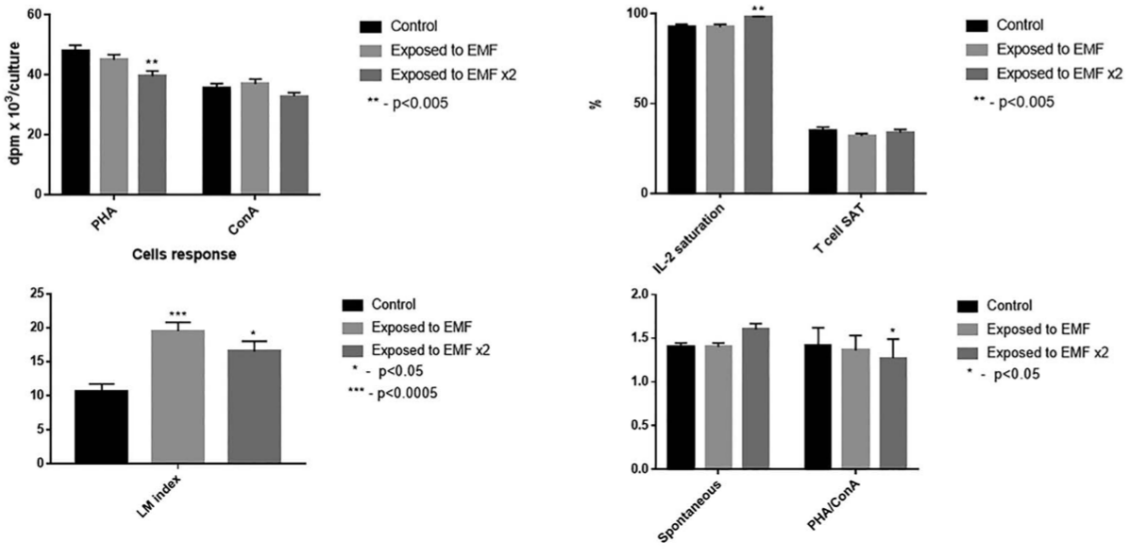


| MEAN ± SEM | Spontaneous n=26 | Response to PHA (dpm x $10^3$/culture) n=21 | Response to Con A (dpm x $10^3$/culture) n=26 | Saturation of IL-2 receptors (%) n=23 | T cell suppressive activity SAT (%) n=26 | LM index n=23 | Mitogen response ratio, PHA/Con A n=26 |
|---|---|---|---|---|---|---|---|
| Control | 1.4 ± 0.045 | 48.1 ± 1.7 | 35.6 ± 1.4 | 92.61 ± 1.4 | 35.3 ± 1.6 | 10.55 ± 1.17 | 1.42 ± 0.2 |
| Exposed to EMF | 1.4 ± 0.045 | 45 ± 1.7 | 36.9 ± 1.6 | 92.65 ± 1.4 | 32 ± 1.3 | 19.5 ± 1.3 | 1.36 ± 0.17 |
| Exposed to EMF x 2 | 1.6 ± 0.065 | 39.5 ± 1.8 | 32.8 ± 1.2 | 97.91 ± 0.5 | 33.9 ± 1.7 | 16.5 ± 1.5 | 1.27 ± 0.22 |
| Statistical significance | EMF vs. Control: p=0.779<br>EMF x2 vs. Control: p=0.127 | EMF vs. Control: p=0.204<br>**EMF x 2 vs. Control: p=0.001** | EMF vs. Control: p=0.543<br>EMF x2 vs. Control: p=0.147 | EMF vs. Control: p=0.89<br>**EMF x2 vs. Control: p=0.004** | EMF vs. Control: p=0.126<br>EMF x2 vs. Control: p=0.552 | **EMF vs. Control: p=0.0002**<br>**EMF x 2vs. Control: p=0.009** | EMF vs. Control: p=0.213<br>**EMF x2 vs. Control: p=0.01** |

**Fig. 5. Influence of the EMF on the activity of T lymphocytes and monocytes in microcultures. Results are presented as mean dpm ± SEM.**

Figure 22: Tools used and E Field Distribution

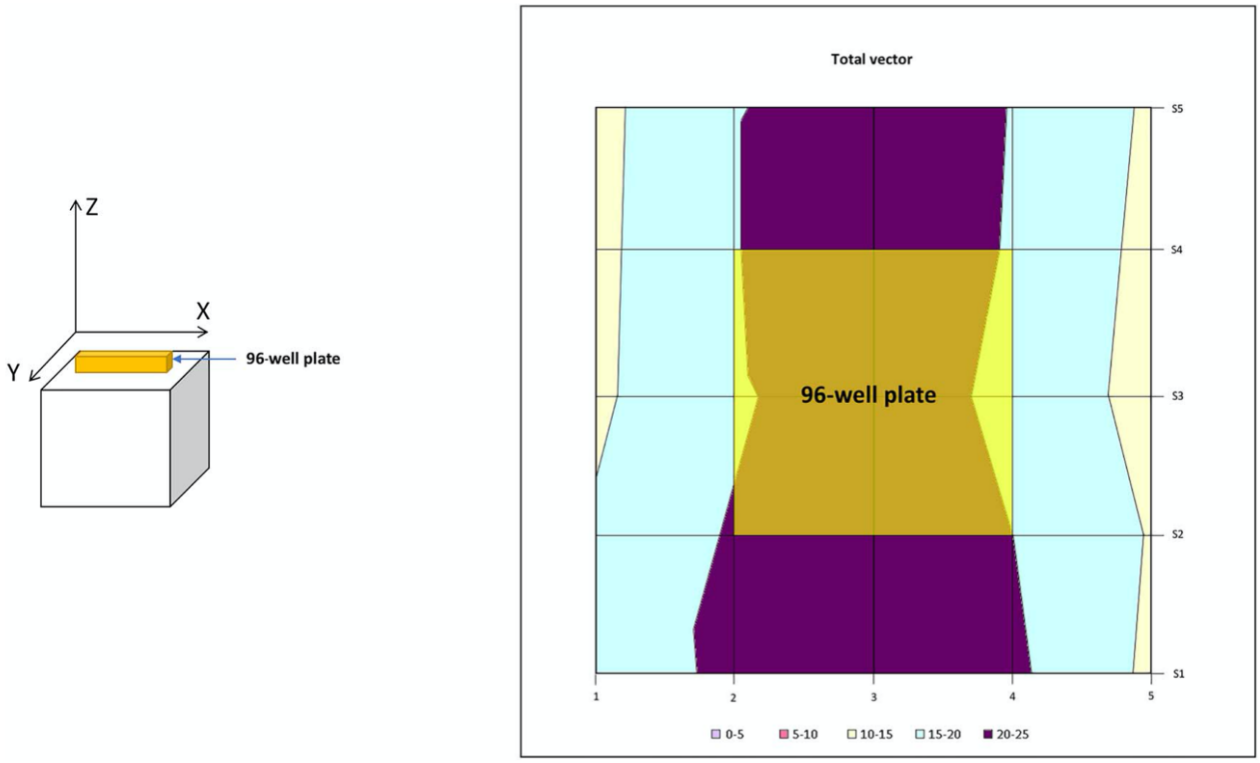


**Fig. 3. The distribution of the electric field strength in the measuring microchamber—900 MHz.**

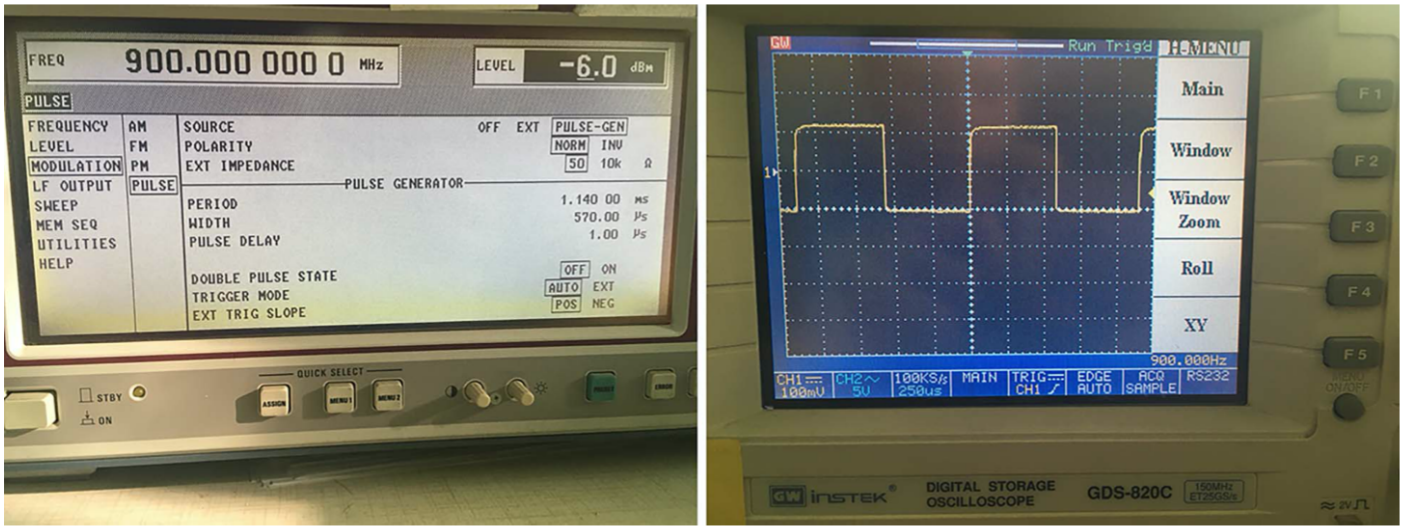


**Fig. 4. Oscilloscope parameters used during examination and envelope excursion of tested signal.**

Figure 23: Schematic Flow Chart for Exposure

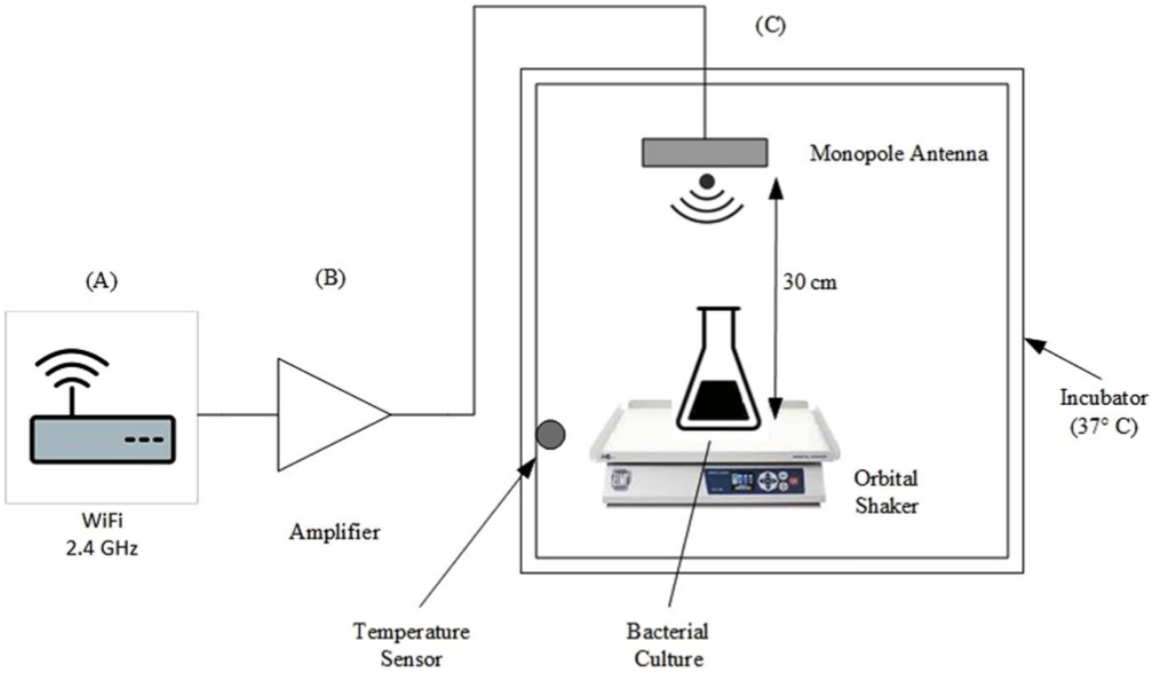


**Figure 9.** Schematic flow chart of the Wi-Fi radiofrequency exposure model. (**A**) Wi-Fi router (**B**) amplifier (**C**) monopole antenna mounted in an incubator chamber with temperature control.

Figure 24: Possible Affected Areas on Bacterial Anatomy and Gene Expression Changes

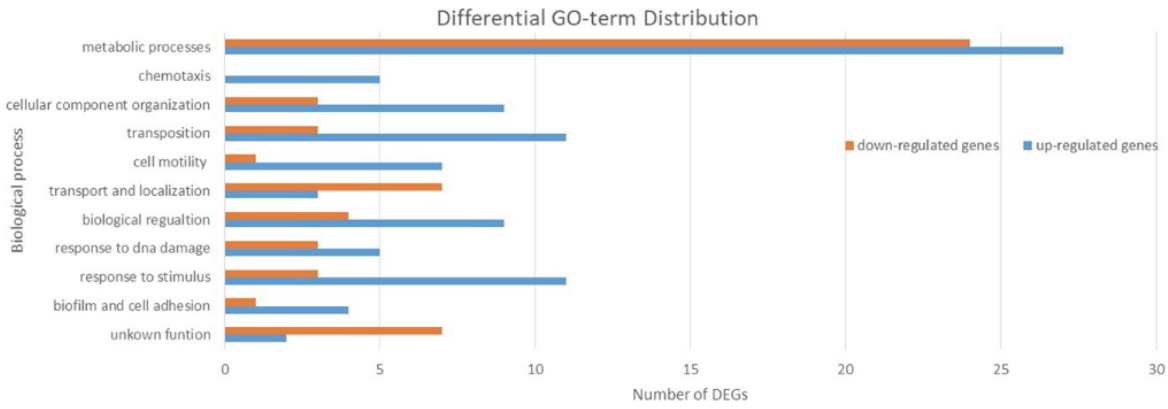


**Figure 4.** GO term enrichment analysis of up- and down-regulated differentially expressed genes.

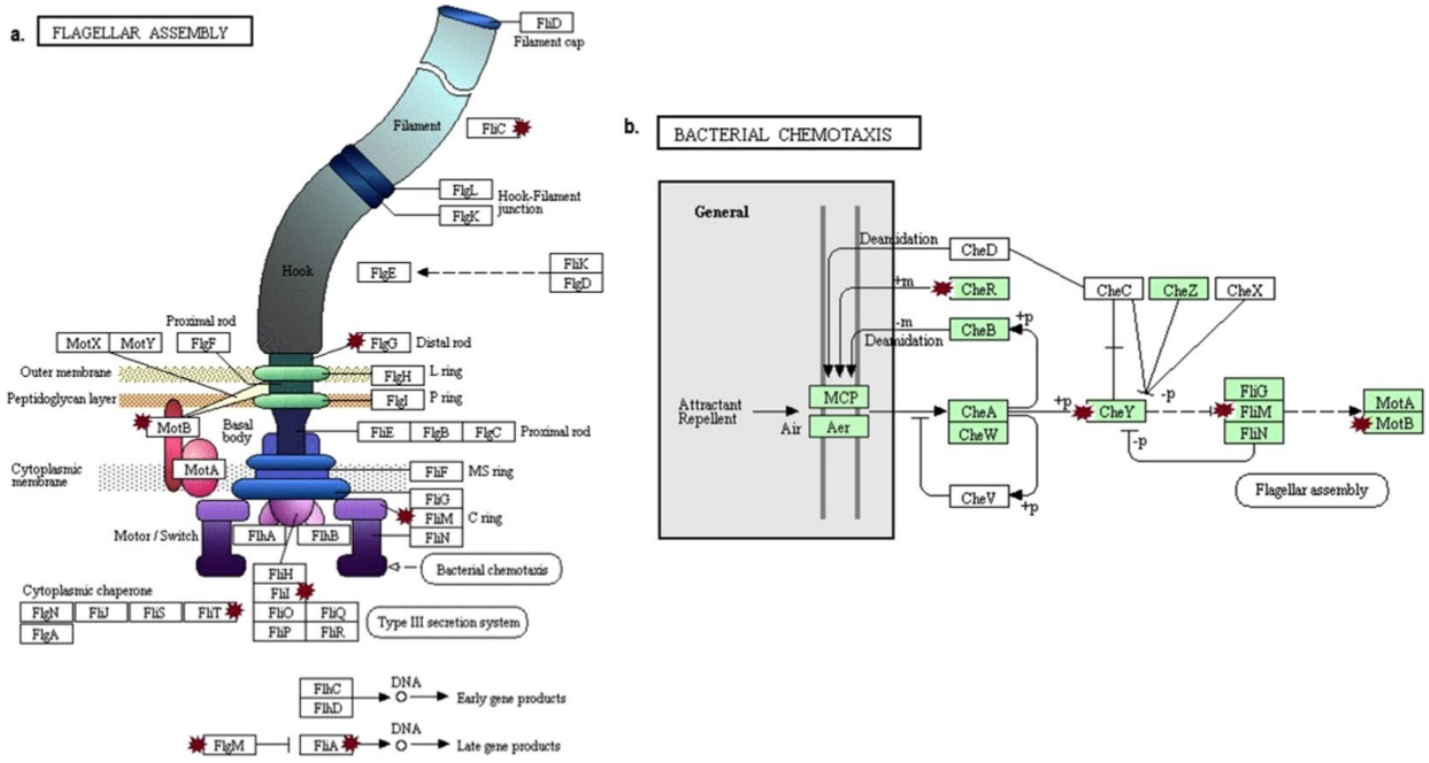


**Figure 5.** Flagellar pathway assembly and bacterial chemotaxis from KEGG database. Red stars point to the up-regulated genes affected in (**a**) the flagelar assembly pathway (ko02040). (**b**) the bacterial chemotaxis pathway (ko02030). Some of the affected genes belong to the two-component system pathway (ko02020).

Figure 25: Possible Pathway for Behavioural Dysfunction After Exposure

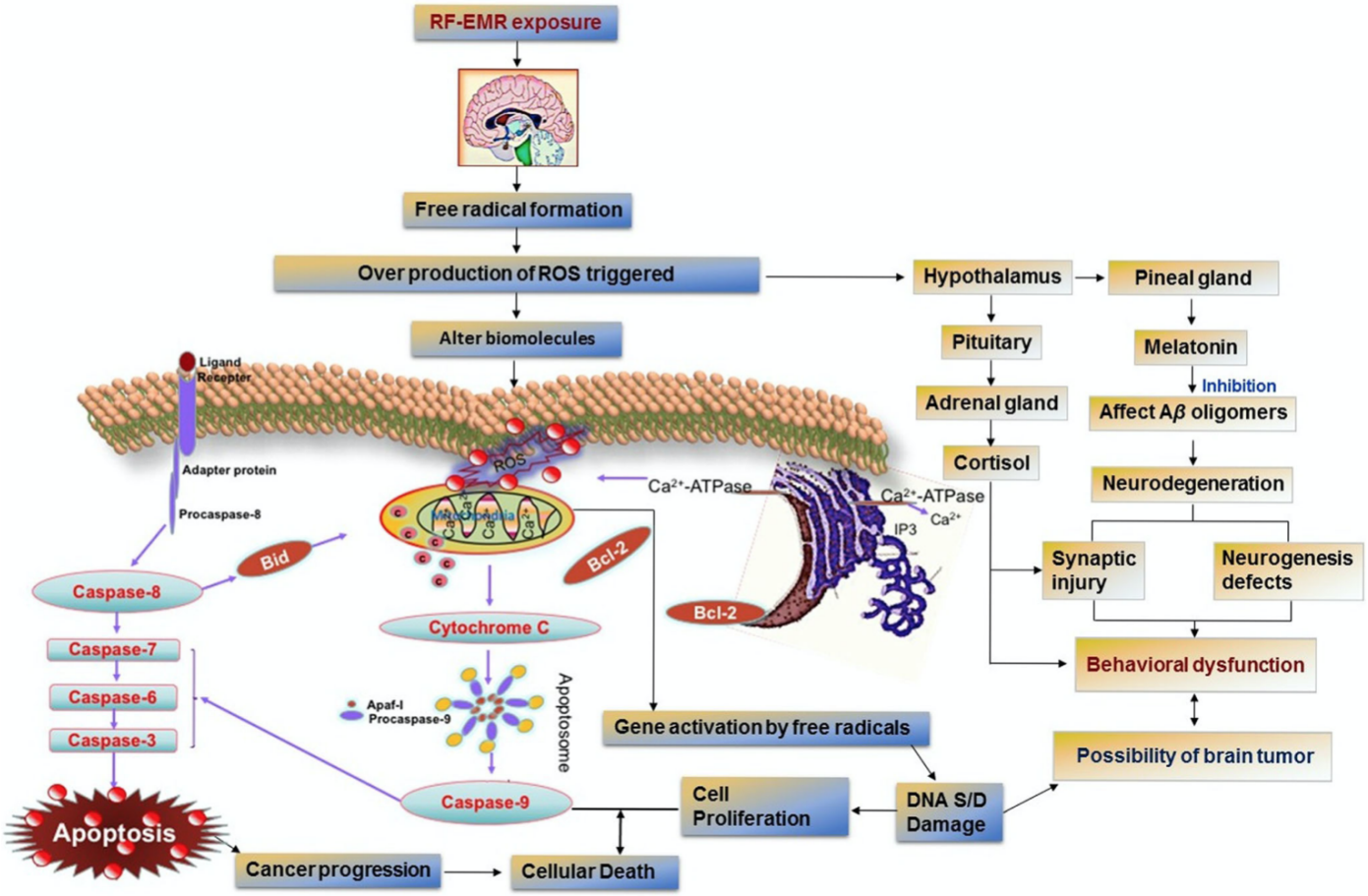


**Fig. 1** Possible pathways leading to behavioral dysfunction and other biological effects in the brain following RF-EMR exposure

Figure 26: Number of Studies Observed and Method

**Table 2.** Overview of the total number of publications examinations.

| All Publications (94) | No Response | Response | All |
|---|---|---|---|
| In vivo | 10 | 35 | 45 |
| In vitro | 22 | 31 | 53 |
| Primary cells | 6 | 18 | |
| Cell lines | 16 | 13 | |

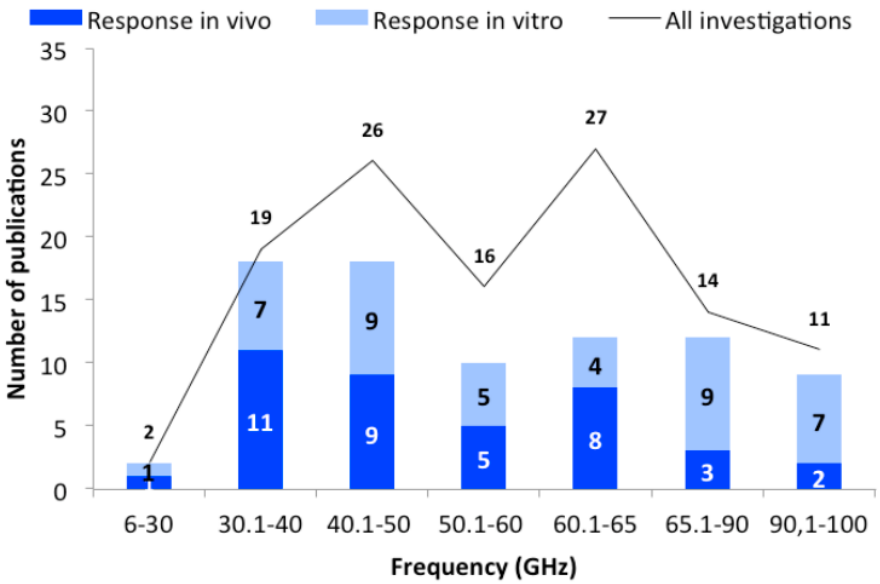


**Figure 1.** The number of publications as a function of frequency domains. The black line represents the total number of publications, and bars represent the in vivo (dark blue) and in vitro (light blue) studies with biological responses.

Figure 27: A breakdown of What the Studies Observed

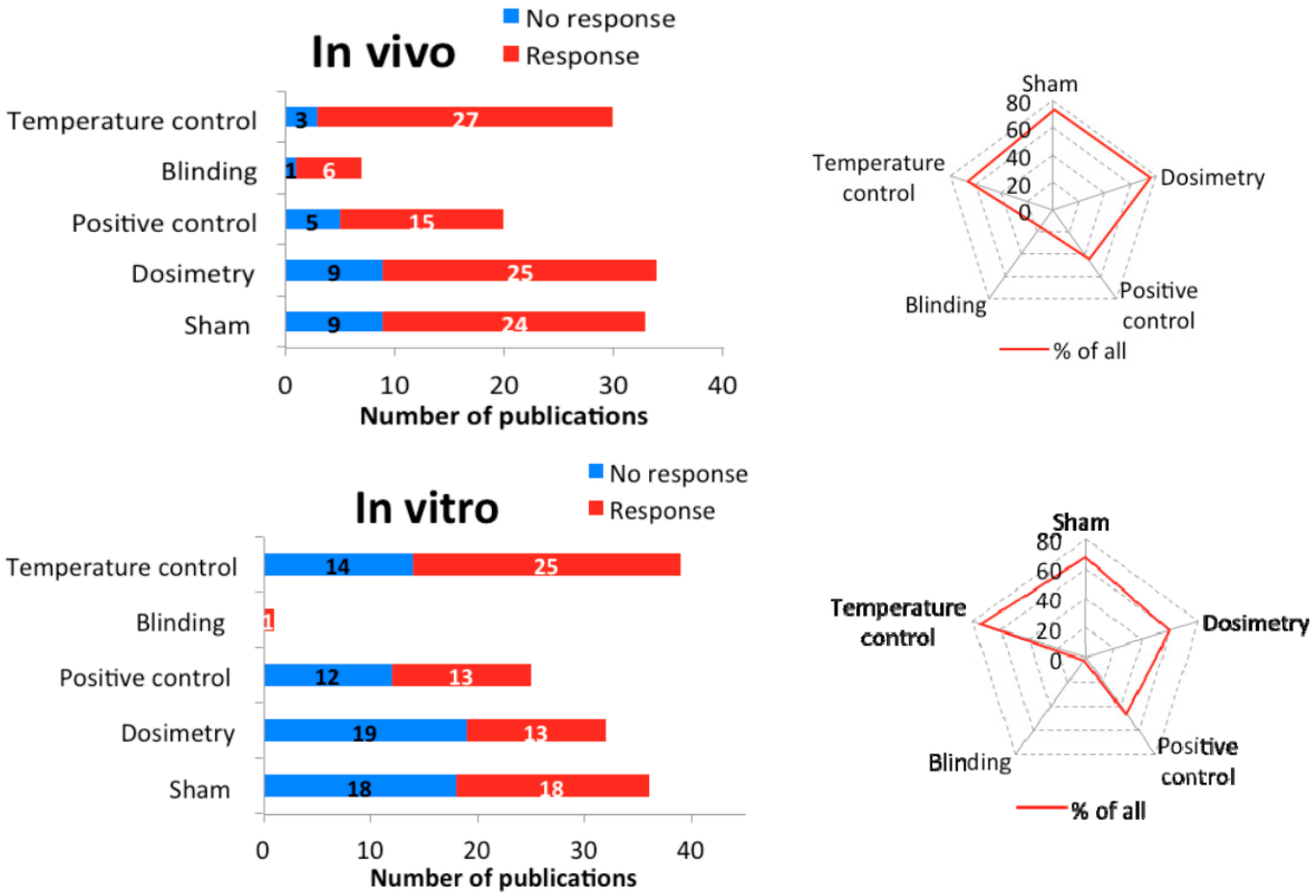


**Figure 4.** The quality of all publications: The number of in vivo (top) and in vitro (bottom) experiments (blue: no reaction, red: reaction) using the listed quality features (y-axis). The spider web shows the percentage of the quality characteristics in all examinations.

Figure 28: Publication Funding Sources

**TABLE 1**
**Number and Percentage of Publications and Tests**

| Funding source | No. of publications (%) | No. of tests (%) |
|---|---|---|
| Government | 120 (53) | 1,227 (57) |
| Industry | 20 (9) | 265 (12) |
| Private | 9 (4) | 33 (2) |
| Government + industry | 10 (4) | 160 (7) |
| Government + private | 8 (4) | 97 (4) |
| Not mentioned | 58 (26) | 378 (18) |
| Total no. of publications and tests | 225 | 2,160 |

Figure 29: Quality Control Measures In Publications

**TABLE 2**
**Quality Control Measures Mentioned in the Publications (%) and Tests (%) Funded by Different Organizations**

| | Government | | Industry | | Private-government-industry | | Not mentioned | |
|---|---|---|---|---|---|---|---|---|
| Quality measure | % (No. pubs) | % (No. tests) | % (No. pubs) | % (No. tests) | % (No. pubs) | % (No. tests) | % (No. pubs) | % (No. tests) |
| B | 63 (76) | 69 (841) | 85 (17) | 96 (254) | 59 (16) | 87 (251) | 47 (27) | 63 (238) |
| nB | 37 (44) | 31 (386) | 15 (3) | 4 (11) | 41 (11) | 13 (39) | 53 (31) | 37 (140) |
| D | 69 (83) | 82 (1009) | 95 (19) | 99 (262) | 93 (25) | 99 (288) | 38 (22) | 56 (211) |
| nD | 31 (37) | 18 (218) | 5 (1) | 1 (3) | 7 (2) | 1 (2) | 62 (36) | 44 (167) |
| P | 62 (74) | 83 (1016) | 80 (16) | 94 (250) | 74 (20) | 80 (233) | 36 (21) | 64 (243) |
| nP | 38 (46) | 17 (211) | 20 (4) | 6 (15) | 26 (7) | 20 (57) | 64 (37) | 36 (135) |
| S | 73 (88) | 19 (234) | 85 (17) | 4 (10) | 74 (20) | 6 (18) | 38 (22) | 37 (138) |
| nS | 27 (32) | 81 (993) | 15 (3) | 96 (255) | 26 (7) | 94 (272) | 62 (36) | 63 (240) |
| Total no. of publications | 120 | | 20 | | 27 | | 58 | |
| Total no. of tests | | 1,227 | | 265 | | 290 | | 378 |

*Note*. B = blind analysis was mentioned; nB = blind analysis was not mentioned; D = dosimetry was adequately described; nD = poor description of dosimetry; P = positive controls were included; nP = positive controls were not mentioned; S = sham-exposed controls were used; nS = sham-exposed controls were not mentioned.

Figure 30: Conclusions of the Publications

**TABLE 4**
**Conclusions in Publications (%) Funded by Different Organizations**

| | Percentage of publications | | | |
|---|---|---|---|---|
| Conclusions | Government | Industry | Private-government-industry | Not mentioned |
| NSD | 49 | 80 | 70 | 34 |
| INC | 23 | 10 | 19 | 31 |
| DEC | 1 | 0 | 0 | 0 |
| MIX | 27 | 10 | 11 | 34 |
| Total no. of publications | 120 | 20 | 27 | 58 |

*Note*. NSD = no significant difference in damage between RF-exposed and sham-exposed cells; INC = significantly increased damage in RF-exposed cells compared to sham-exposed cells; DEC = significantly decreased damage in RF-exposed cells; MIX = significant increase, significant decrease and no significant damage in RF-exposed cells compared to sham-exposed cells.

Figure 31: MSCs DNA Damage

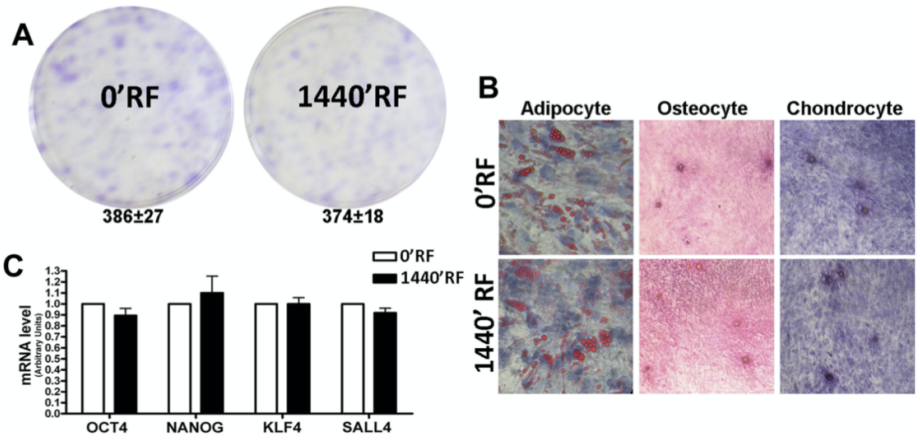


**Figure 2** Stemness properties of Mesenchymal Stem Cells (MSCs) after Radiofrequency (RF) exposure. (**A**) The pictures show representative crystal violet staining of clones obtained after 14 days of incubation with MSCs following RF exposure. The mean number of clones per 1000 cells plated in 100 mm dish (± SD, n=3). (**B**) Microscope images of MSCs differentiated in: adipocyte evaluated by Oil Red O staining; osteocyte evaluated by Alizarin red S (ARS) staining and chondrocyte evaluated by Safranin O staining. (**C**) Histograms show expression levels of the mRNA of the gene as indicated. The mRNA levels were normalized to GAPDH mRNA expression, which was selected as an internal control. Data are expressed as arbitrary units with standard deviation (n=3).

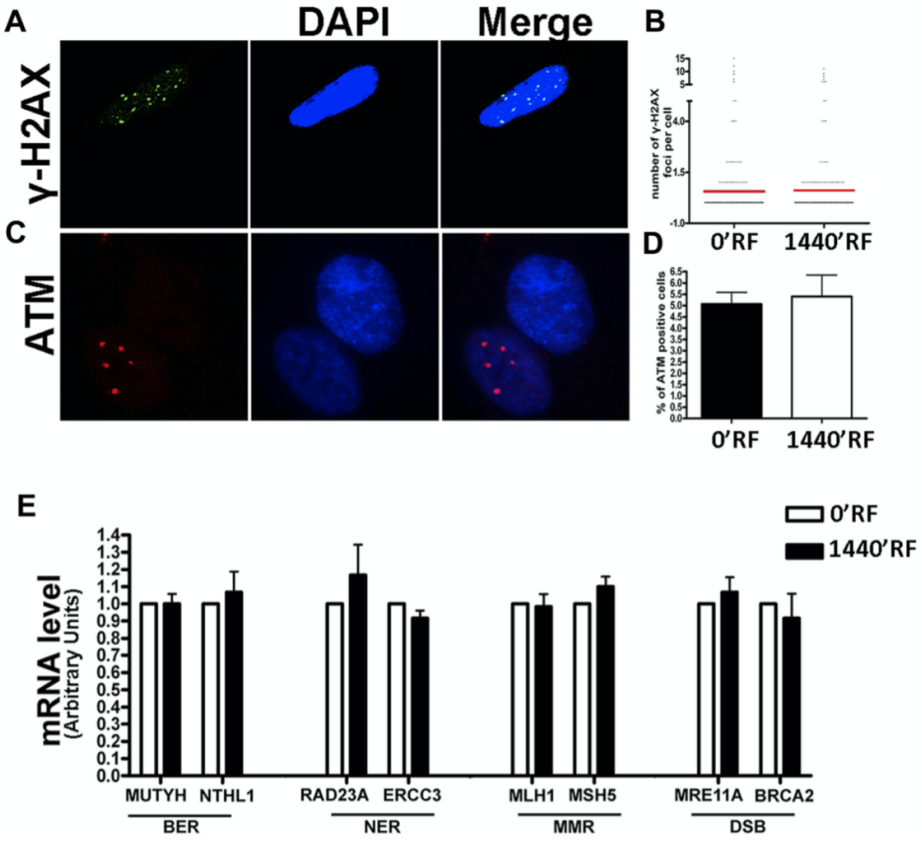


**Figure 3** DNA damage and repair analysis. (**A**) Fluorescence photomicrographs show the merging of cells stained with anti-H2AX (green). Nuclei were counterstained with DAPI (blue). A representative microscopic field for each treatment is shown. (**B**) Graph shows the degree of H2AX phosphorylation. This was evaluated by counting the number of gamma-H2AX immunofluorescent foci per cell. Foci number was determined for 200 cells. Each dot represents an individual cell. Black bars indicate mean value for each category (n=3). (**C**) Fluorescence photomicrographs show typical cells stained with anti-ATM (green) and DAPI (Blue). A representative microscopic field for each treatment is shown. (**D**) The graph indicates the mean percentage of ATM-positive cells for each condition. The data are indicated with standard deviation (n=3). (**E**) Histograms show expression levels of the mRNA of the gene as indicated. The mRNA levels were normalized to GAPDH mRNA expression, which was selected as an internal control. Data are expressed as arbitrary units with standard deviation (n=3).

## References


[1] N. Alessio, E. Santoro, T. Squillaro, D. Aprile, M. Briccola, P. Giubbini, R. Marchesani, M. Muoio, and M. Lamberti. Low-level radiofrequency exposure does not induce changes in msc biology: An in vitro study for the prevention of nir-related damage. *Stem Cells and Cloning : Advances and Applications*, 12:49–59, 2019.

[2] M. E. Alkis, H. M. Bilgin, V. Akpolat, S. Dasdag, K. Yegin, M. C. Yavas, and M. Z. Akdag. Effect of 900-, 1800-, and 2100-mhz radiofrequency radiation on dna and oxidative stress in brain. *Electromagnetic Biology and Medicine*, 38(1):32–47, 2019.

[3] J. H. Kim, Y. H. Huh, and H. R. Kim. Trafficking of synaptic vesicles is changed at the hypothalamus by exposure to an 835 mhz radiofrequency electromagnetic field. *Gen Physiol Biophys*, 38(5):379–388, 2019.

[4] R. N. Kostoff, P. Heroux, M. Aschner, and A. Tsatsakis. Adverse health effects of 5g mobile networking technology under real-life conditions. *Toxicol Lett*, 323:35–40, 2020.

[5] L. Migault, J. D. Bowman, H. Kromhout, J. Figuerola, I. Baldi, G. Bouvier, M. C. Turner, E. Cardis, and J. Vila. Development of a job-exposure matrix for assessment of occupational exposure to high-frequency electromagnetic fields (3 khz-300 ghz). *Annals of work exposures and health*, 63(9):1013–1028, 2019.

[6] S. Narayanan, R. Jetti, K. Kesari, R. Kumar, S. B. Nayak, and P. G. Bhat. Radiofrequency electromagnetic radiation-induced behavioral changes and their possible basis. *Environmental Science And Pollution Research*, 26(30):30693–30710, 2019.

[7] C. Nielsen, R. Hui, W.-Y. Lui, and I. A. Solov'yov. Towards predicting intracellular radiofrequency radiation effects.(research article). *PLoS ONE*, 14(3):e0213286, 2019.

[8] I. Said-Salman, F. A. Jebaii, H. Hyusef, and M. E. Moustafa. Global gene expression analysis of escherichia coli k-12 dh5 alpha after exposure to 2.4 ghz wireless fidelity radiation. *Scientific Reports*, 9(1), 2019.

[9] M. Simkó and M.-O. Mattsson. 5g wireless communication and health effects-a pragmatic review based on available studies regarding 6 to 100 ghz. *International journal of environmental research and public health*, 16(18), 2019.

[10] L. Szymanski, E. Sobiczewska, A. Cios, P. Szymanski, M. Ciepielak, and W. Stankiewicz. Immunotropic effects in cultured human blood mononuclear cells exposed to a 900 mhz pulse-modulated microwave field. *J Radiat Res*, 61(1):27–33, 2020.

[11] Vijayalaxmi and T. J. Prihoda. Funding source, quality of publications and outcome in genetic damage in mammalian cells exposed to non-ionizing radiofrequency fields. *Radiat Res*, 192(4):353–362, 2019.